patient developed new lesions and died on day 71. These patients were included in the analysis as a responder and a nonresponder, respectively. The overall response rate was 53%. Forty-one patients died, and the median follow-up time for the 25 survivors was 14.6 months (range, 10.3 to 32.3 months). Eleven patients were still receiving gefitinib without progression at the time of the analysis. The median TTP and the median survival time (MST) for all patients were 5.2 and 16.3 months, respectively.

EGFR *and* ERBB2 *Mutations*

Forty-three mutations in the *EGFR* tyrosine kinase domain were detected in 39 (59%) of the 66 patients. All the mutations detected in this study are shown in Table 2. Twenty patients had deletional mutations in exon 19, and 17 patients had missense mutations (L858R) in exon 21. In exons 18 and 20, five types of missense mutations were detected. Two of them (G719S and G719C) occurred at a codon considered to be a third hotspot.[6,7,9-12] The others (L703V, E709K, and S768I) were detected in patients who also had mutations at the hotspots. Because these mutations were not detected in the normal lung tissues from the same patients, they were considered to be somatic mutations. No somatic mutations were detected in exons 22 to 24. Silent single nucleotide polymorphisms were identified at nucleotides 2361 (G/A; Q787Q), 2370 (G/A; T790T), and 2457 (G/A; V819V) in exon 20, and at nucleotide 2709 (C/T; T903T) in exon 23, but the association between these polymorphisms and the somatic mutations was not observed. In this study, no mutations and no polymorphisms were detected in exons 18 to 24 of *ERBB2*.

All 43 mutations were detected in LCM samples, but 11 (26%) of these mutations were not detected in the bulk tumor samples. In 13 patients, LCM was performed at separate areas with different histologic subtypes, but no heterogeneity was identified; the same mutations were detected in nine patients, and no mutations were detected in four patients. Mutational analyses of synchronous double lung cancers were performed in two patients; one patient had a tumor with wild-type *EGFR* and a more invasive tumor with L858R + S768I, and the other patient had a tumor with a 9-bp deletion (del L747-E749) and a more invasive tumor with a 15-bp deletion (del E746-T751insA) + L703V.

Among the 39 patients with *EGFR* mutations, the proportion of mutant alleles ranged from 29% to 94%. Nineteen patients showed a BH pattern and 20 patients showed an MD pattern.

EGFR *Copy Number*

The *EGFR* copy number in the laser-captured tumor cells ranged from 1.27 to 31.2 per cell, and increased *EGFR* copy numbers (≥ 3.0 per cell) were observed in 29 patients (44%). The relation between the copy number and the proportion of mutant alleles is shown in Figure 1. Increased copy numbers were observed more frequently in patients with *EGFR* mutations than in patients with wild-type *EGFR* (56% [22 of 39 patients] *v* 26% [seven of 27 patients]; $P = .014$). High copy numbers (≥ 6.0 per cell) were observed only in patients with an MD pattern of mutations. The copy number and the proportion of mutant alleles among patients with *EGFR* mutations was positively correlated (Spearman correlation coefficient = 0.643; $P < .001$), implying that the mutant alleles were selectively amplified in patients with an MD pattern. One patient with an MD pattern had a tumor with only approximately one copy per cell, indicating a hemizygous mutation with a loss of wild-type allele. No alterations in the gene copy number were observed in normal lung tissues.

Table 2. *EGFR* Mutations Detected in the Present Study

Exons	Amino Acids	Nucleotides	No. of Patients
19	del E746-A750	del 2235-2249	12
	del E746-A750	del 2236-2250	5
	del E746-T751insA	del 2237-2251	1
	del L747-E749	del 2239-2247	1
	del E746-S752insV	del 2237-2255 + ins T	1
21	L858R	T → G at 2573	17
18	G719S	G → A at 2155	1
	G719C	G → T at 2155	1
	L703V	C → G at 2107	1*
	E709K	G → A at 2125	1†
20	S768I	G → T at 2303	2‡

Abbreviations: *EGFR*, epidermal growth factor receptor; del, deletion; ins, insertion.
*A patient with del E746-T751insA.
†A patient with L858R.
‡A patient with L858R and a patient with G719C.

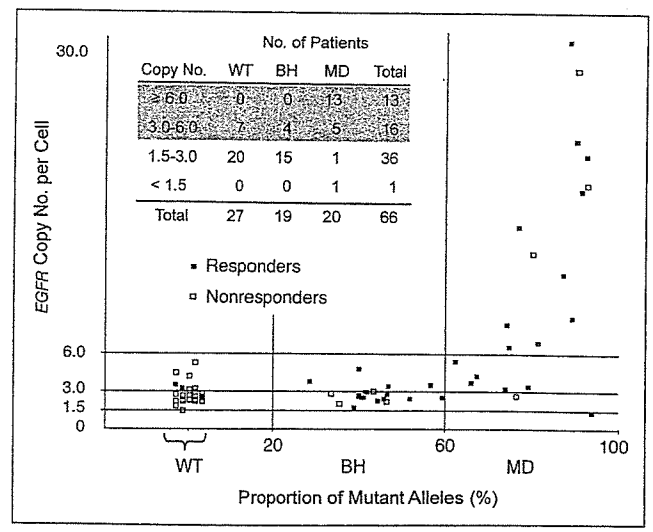

Fig 1. Relation between the epidermal growth factor receptor (*EGFR*) copy number and the proportion of mutant alleles. WT, patients with wild-type *EGFR*; BH, patients with a balanced heterozygous pattern of *EGFR* mutations; MD, patients with a mutant-allele-dominant pattern of *EGFR* mutations.

EGFR *Mutations,* EGFR *Copy Number, and Clinical Outcome*

The tumor responses to gefitinib according to the mutational status of *EGFR* are shown in Table 3. The response rates of patients with mutant and wild-type *EGFR* were 82% and 11%, respectively ($P < 10^{-7}$). Seven patients with *EGFR* mutations were nonresponders; three patients had PD at 0.3 (early death), 2.3, and 2.3 months, and four patients had SD. Three of the four patients with SD had MR (TTP, 2.5, 5.2, and 6.9 months), and the other patient continued to receive gefitinib therapy without progression for 24.2 months, whereas all SD tumors with wild-type *EGFR* progressed within 5 months without MR. Meanwhile, three patients with wild-type *EGFR* exhibited PR, and two of these patients were still receiving gefitinib therapy without progression at 10.9+ and 21.1+ months. The Kaplan-Meier plots of TTP and OS according to the presence of the *EGFR* mutations are shown in Figures 2 and 3, respectively. Patients with *EGFR* mutations had a significantly longer TTP and OS compared with those with wild-type *EGFR*.

Univariate analyses were performed to assess the correlations among patient characteristics, *EGFR* mutations, *EGFR* copy number, and clinical outcome (Tables 4 and 5). The response rates were significantly higher in women, never/former smokers, and patients with BAC features and were marginally higher in patients with a papillary-dominant subtype. The response rates among these subgroups were approximately consistent with the rates of *EGFR* mutations. An increased *EGFR* copy number was also significantly associated with a higher response rate and a longer TTP.

The results of multivariate analyses among 62 patients with adenocarcinoma are shown in Table 6. The presence of *EGFR* mutations was strongly associated with a higher response rate, a longer TTP, and a longer OS. An increased *EGFR* copy number was also a significant or marginally significant predictor of a higher response rate and a longer TTP. These results did not change substantially if any combinations of variables were included in the models.

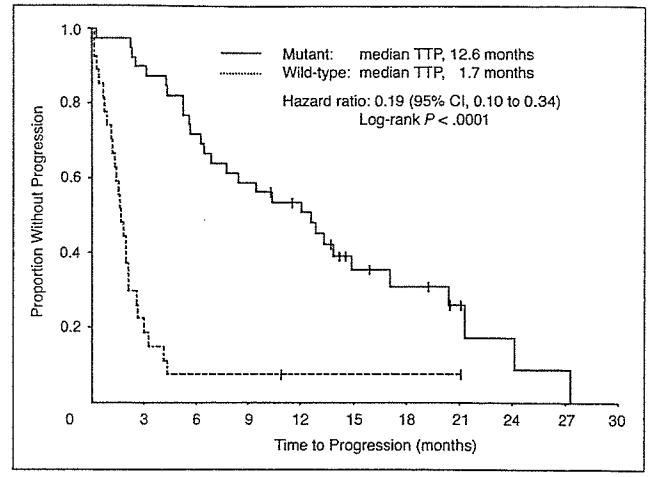

Fig 2. Kaplan-Meier plot of time to progression (TTP) according to epidermal growth factor receptor (*EGFR*) mutation status.

Among patients with wild-type *EGFR*, TTP was significantly longer in patients with increased *EGFR* copy numbers (median, 3.0 *v* 1.4 months; log-rank $P = .021$), and both of the two long-term responders had tumors with moderately increased *EGFR* copy numbers (3.20 and 3.45/cell). Among patients with *EGFR* mutations, TTP and OS were not significantly different according to the types of mutations, the presence of additional mutations, the proportion of mutant alleles, or the *EGFR* copy number (data not shown).

DISCUSSION

This study strongly implies that the mutational status of *EGFR* is a major determinant of gefitinib sensitivity in patients with NSCLC. The response rate was 82%, the median TTP was 12.6 months, and the MST was 20.4 months in gefitinib-treated patients with *EGFR*-mutant NSCLC. *EGFR* mutations might be a good prognostic factor independent of treatment, but these remarkable results suggest a

Table 3. *EGFR* Mutations and Tumor Response to Gefitinib

	Responders		Nonresponders			Responders/Total Patients	Response Rates (%)
	CR	PR	MR	SD	PD		
Mutant	2	30*	3	1	3†	32/39	82
DEL	0	18*	2	0	0	18/20	90
L858R	2	11	1	1	2†	13/17	76
G719	0	1	0	0	1	1/2	50
Wild-type	0	3	0	5	19	3/27	11
Total	2	33	3	6	22	35/66	53

Abbreviations: *EGFR*, epidermal growth factor receptor; CR, complete response; PR, partial response; MR, minor response; SD, stable disease without MR; PD, progressive disease; DEL, deletional mutations in exon 19; G719, G719S, or G719C.
*Including a clinical responder without measurable lesions.
†Including a patient who had no measurable lesions at baseline.

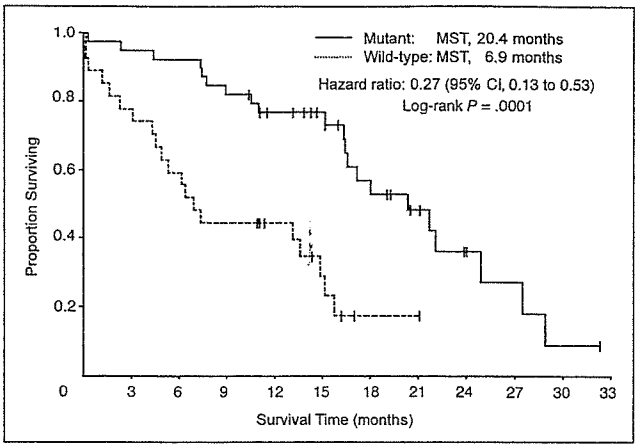

Fig 3. Kaplan-Meier plot of overall survival according to epidermal growth factor receptor (*EGFR*) mutation status. MST, median survival time.

survival benefit from gefitinib therapy in patients with *EGFR* mutations. Four of seven nonresponders with *EGFR* mutations also seemed to experience some clinical benefits because they had MR or a long SD (≥ 6 months). Among nine patients with SD, MR, or a long SD was observed only in patients with *EGFR* mutations. Although the sample size was too small to draw a firm conclusion, this finding suggests that *EGFR* mutations are also associated with clinical benefits in SD.

Table 4. *EGFR* Mutations Among Patient Subgroups

	EGFR Mutations		
	No. of Patients	%	*P*
Total	39/66	59	
Sex			.18
Female	18/26	69	
Male	21/40	53	
Smoking history			.003†
Never smokers	21/31	68	
Former smokers	10/12	83	
Current smokers	8/23	35	
Histologic diagnosis			—
Adenocarcinoma	38/62	61	
Squamous cell carcinoma	0/3	0	
Pleomorphic carcinoma	1/1	100	
Dominant subtype*			.059‡
Papillary	22/30	73	
Acinar	10/18	56	
BAC	5/9	56	
Solid	1/5	20	
BAC features*			.002
Yes	34/47	72	
No	4/15	27	

Abbreviations: *EGFR*, epidermal growth factor receptor; BAC, bronchioloalveolar carcinoma.
*Only patients with adenocarcinoma (n = 62).
†Comparison between never/former smokers and current smokers.
‡Comparison between patients with papillary-dominant adenocarcinoma and patients with other adenocarcinoma.

The *EGFR* mutations detected in this study were concentrated in three hotspots, deletions around codons 747 to 749, L858R, and G719S (or G719C), similar to the results of previous reports.[6-13] Some genetic variations existed among these mutations. Together with one of the hotspot mutations, additional missense mutations in exons 18 or 20 were detected in four patients. Among the 39 patients with *EGFR* mutations, an MD pattern was observed in 20 patients. Because the *EGFR* copy number in their tumor cells increased as the proportion of mutant alleles increased, this pattern was assumed to be caused not by homozygous mutations but by the selective amplification of the mutant alleles. Because one patient had a hemizygous mutation without amplification, the loss of wild-type alleles was also thought to be responsible for the pattern. The moderately increased copy number in patients with a BH pattern or wild-type *EGFR* can be explained by *EGFR* amplification and/or polysomy of chromosome 7.

Among the patients with *EGFR* mutations, three patients had PD and eight of the other 36 patients had tumor regrowth within 6 months. This suggests the presence of other factors associated with intrinsic or acquired resistance to gefitinib. Although any genetic alterations of *EGFR*-mutant tumors at the time of primary surgery were not significantly associated with clinical outcome, that might be because further alterations occurred after the primary surgery or after gefitinib administration. Recently, a secondary mutation (C → T at nucleotide 2369; T790M) in exon 20 was detected in patients with *EGFR*-mutant NSCLC who had tumor regrowth during gefitinib therapy after exhibiting an initial response to the agent; this mutation was thought to be associated with acquired resistance.[28,29] To elucidate the determinants and the mechanism of resistance to gefitinib, genetic analyses of tumor samples obtained after gefitinib treatment are needed.

In this study, three (11%) of the 27 patients with wild-type *EGFR* responded to gefitinib. Various explanations for this result are possible: (1) the mutational analyses of the responders were false-negative, (2) the *EGFR* mutations occurred in their tumors after the primary surgery, (3) the recurrent tumors originated from a source other than the analyzed tumor cells, or (4) other determinants of gefitinib sensitivity were present.

The results of multivariate analyses suggest that the *EGFR* copy number is another independent predictor of gefitinib sensitivity. It is noteworthy that an increased *EGFR* copy number was observed in two of the three responders with wild-type *EGFR*, and was significantly associated with a longer TTP among patients with wild-type *EGFR*. Because patients with *EGFR* mutations had favorable clinical outcome regardless of *EGFR* copy numbers, the impact of increased copy numbers on *EGFR*-mutant NSCLC was unclear. In the overall population, an increased *EGFR* copy number was significantly associated with a higher response

Table 5. Clinical Outcome Among Patient Subgroups (univariate analyses)

	Response Rate			Time to Progression		Overall Survival	
	No.	%	*P*	Median (months)	Log-Rank *P*	Median (months)	Log-Rank *P*
Total	66	53		5.2		16.3	
Sex			.033		.35		.30
Female	26	69		6.2		16.5	
Male	40	43		3.3		15.1	
Smoking history			.007		.026		.37
Never/former smokers	43	65		6.9		16.4	
Current smokers	23	30		2.6		15.1	
Dominant subtype*			.070		.28		.65
Papillary	30	67		7.7		16.4	
Others	32	44		4.2		15.7	
BAC features*			.012		.12		.19
Yes	47	64		6.5		16.5	
No	15	27		2.1		15.7	
Performance status			.77		.012		< .0001
0-1	50	52		5.2		17.1	
2-3	16	56		3.1		6.1	
EGFR mutations			< .0001		< .0001		.0001
Yes	39	82		12.6		20.4	
No	27	11		1.7		6.9	
EGFR copy number			.005		.038		.33
≥ 3.0	29	72		9.4		16.4	
< 3.0	37	38		2.6		15.7	

Abbreviation: BAC, bronchioloalveolar carcinoma; *EGFR*, epidermal growth factor receptor.
*Only patients with adenocarcinoma (n = 62).

rate and a longer TTP, but not with a longer OS, which might be because an increased copy number had an unfavorable impact on prognosis, as suggested by another study.[15] In chronic myeloid leukemia, as well as *BCR-ABL* mutations that were structurally corresponding to T790M in *EGFR*, an increased *BCR-ABL* gene copy number was reported as a determinant of resistance to imatinib, a BCR-ABL tyrosine kinase inhibitor.[30] Therefore, we should consider the possibility that an increased *EGFR* copy number is associated with not only sensitivity but also resistance to gefitinib.

Among adenocarcinomas, the presence of BAC features was significantly associated with gefitinib sensitivity and *EGFR* mutations, but the BAC component was relatively small in most of the responders. The dominant subtype associated with a higher response rate was not BAC but papillary; both of the two patients with BwFI had PD, and all three patients with pure papillary adenocarcinoma without BAC features had PR. The association between pathologic features and gefitinib sensitivity or *EGFR* mutations is also the subject of further investigation.

Table 6. Univariate and Multivariate Analyses of the Association Between Biomarkers and Clinical Outcome in Patients With Lung Adenocarcinoma (n = 62)

	Odds Ratios for Response		Hazard Ratios for TTP		Hazard Ratios for OS	
	Univariate	Multivariate*	Univariate	Multivariate*	Univariate	Multivariate*
EGFR mutations, yes *v* no	31.0	27.9	0.21	0.13	0.30	0.16
95% CI	7.2 to 134	3.7 to 209	0.11 to 0.38	0.06 to 0.29	0.15 to 0.62	0.06 to 0.39
P	< .001	.001	< .001	< .001	.001	< .001
EGFR copy number, ≥ 3.0 *v* < 3.0	4.0	4.6	0.57	0.42	0.80	0.59
95% CI	1.4 to 12	0.84 to 25	0.32 to 1.0	0.21 to 0.84	0.42 to 1.5	0.26 to 1.4
P	.011	.079	.050	.014	.49	.22

Abbreviations: TTP, time to progression; OS, overall survival; *EGFR*, epidermal growth factor receptor.
*In the multivariate analyses, age (continuous variable), sex (women *v* men), smoking history (never/former smokers *v* current smokers), dominant subtype (papillary *v* others), bronchioloalveolar carcinoma features (yes *v* no), performance status (0 to 1 *v* 2 to 3), prior chemotherapy (yes *v* no), *EGFR* mutations (yes *v* no), and *EGFR* copy number (≥ 3.0 *v* < 3.0) were included as factors.

In never/former smokers, both the *EGFR* mutation rate and the response rate were significantly higher than in current smokers. We speculate that *EGFR* mutations occur equally throughout the entire population, regardless of smoking history, and account for smoking-unrelated carcinogenesis. Because many other genetic alterations, like *KRAS* mutations, occur and induce lung adenocarcinoma more frequently in smokers, the *EGFR* mutation rate seems to be relatively lower in smokers with lung adenocarcinoma.

The response rate of 53% and the *EGFR* mutation rate of 59% observed in this study were higher than previously reported rates. These results can partially be attributed to the fact that the physicians tended to select patients with characteristics known to be predictive for gefitinib sensitivity: women, never-smokers, and patients with adenocarcinoma. Consequently, this cohort was not necessarily representative of unselected NSCLC populations in Japan. However, other recent studies have also shown relatively high frequencies (32% to 55%) of *EGFR* mutations in Japanese or East Asian patients with lung adenocarcinoma who underwent surgical resection.[7,9-11,13] The reason why such somatic mutations occur selectively in East Asian people remains unknown. Environmental or genetic factors common among East Asian populations should be investigated to answer this question.

Recently, no significant survival benefit of gefitinib was reportedly observed in the initial analysis of the IRESSA Survival Evaluation in Lung Cancer (ISEL) trial, a phase III trial comparing gefitinib monotherapy to a placebo as a second- or third-line treatment for patients with advanced NSCLC.[31] Because subgroup analyses of the trial suggested survival benefits in never smokers or Asian patients, the selection of patients is thought to be crucial when considering gefitinib treatment. Because the present study showed that the *EGFR* mutation status is a major determinant of gefitinib sensitivity, mutational analyses in patients with advanced NSCLC should be considered before deciding on a course of treatment.

In this study, we performed LCM and direct sequencing using methanol-fixed surgical specimens to obtain high-quality data. If we had analyzed only bulk tumor samples without LCM, nine of the 39 patients with *EGFR* mutations would have been misjudged as having wild-type *EGFR*. Thus such procedures with LCM are presently recommended for the detection of *EGFR* mutations. However, obtaining appropriate tumor samples is often difficult in patients with advanced NSCLC, and performing LCM and direct sequencing in all patients is not practical. Thus more practical methods for detecting the major *EGFR* mutations using small tumor samples contaminated with normal tissue should be developed and validated.

Other than *EGFR* mutations, some candidate predictive biomarkers have been studied. The *EGFR* copy number is the leading candidate, and it can also be detected by FISH. Practicality and accuracy should be assessed comparing FISH and quantitative real-time PCR. The impact of *ERBB2* mutations on clinical outcome remains to be investigated because we could not detect any mutations in *ERBB2* in the present study. Protein expression analyses by IHC are easier to perform than the genetic analyses, but their significance is still controversial. Further studies are required to evaluate the predictive values of these biomarkers and to determine whether they are independent predictors of gefitinib sensitivity or surrogate markers of *EGFR* mutations.

In conclusion, this study indicates that *EGFR* mutations and increased copy numbers predict better clinical outcome in patients with NSCLC treated with gefitinib. Further research and clinical trials are needed to incorporate these markers into clinical practice appropriately.

Acknowledgment

We thank Yukihiro Yoshida, MD; Shunichi Watanabe, MD; Kenji Suzuki, MD; Hisao Asamura, MD; and Ryosuke Tsuchiya, MD, for providing surgical specimens and helpful advice, and Chizu Kina, Chie Hirama, Sanae Kobayashi, Yasuko Kuwahara, Go Maeno, Sachiyo Mimaki, Yoko Odaka, Shizuka Shinohara, Takahiro Taniguchi, and Mineko Ushiama for LCM and DNA analysis. We also thank Setsuo Hirohashi, MD, for his invaluable direction and support of the study.

Authors' Disclosures of Potential Conflicts of Interest

The authors indicated no potential conflicts of interest.

REFERENCES

1. Fukuoka M, Yano S, Giaccone G, et al: A multi-institutional randomized phase II trial of gefitinib for previously treated patients with advanced non-small cell lung cancer (The IDEAL 1 Trial). J Clin Oncol 21:2237-2246, 2003

2. Kris MG, Natale RB, Herbst RS, et al: Efficacy of gefitinib, an inhibitor of the epidermal growth factor receptor tyrosine kinase, in symptomatic patients with non-small cell lung cancer: A randomized trial. JAMA 290:2149-2158, 2003

3. Miller VA, Kris MG, Shah N, et al: Bronchioloalveolar pathologic subtype and smoking history predict sensitivity to gefitinib in advanced non–small-cell lung cancer. J Clin Oncol 22:1103-1109, 2004

4. Takano T, Ohe Y, Kusumoto M, et al: Risk factors for interstitial lung disease and predictive factors for tumor response in patients with advanced non-small cell lung cancer treated with gefitinib. Lung Cancer 45:93-104, 2004

5. Kim YH, Ishii G, Goto K, et al: Dominant papillary subtype is a significant predictor of the response to gefitinib in adenocarcinoma of the lung. Clin Cancer Res 10:7311-7317, 2004

6. Lynch TJ, Bell DW, Sordella R, et al: Activating mutations in the epidermal growth factor receptor underlying responsiveness of non–small-cell lung cancer to gefitinib. N Engl J Med 350:2129-2139, 2004

7. Paez JG, Janne PA, Lee JC, et al: *EGFR* mutations in lung cancer: Correlation with clinical response to gefitinib therapy. Science 304:1497-1500, 2004

8. Pao W, Miller V, Zakowski M, et al: EGF receptor gene mutations are common in lung cancers from "never smokers" and are associated with sensitivity of tumors to gefitinib and erlotinib. Proc Natl Acad Sci U S A 101:13306-13311, 2004

9. Kosaka T, Yatabe Y, Endoh H, et al: Mutations of the epidermal growth factor receptor gene in lung cancer: Biological and clinical implications. Cancer Res 64:8919-8923, 2004

10. Huang SF, Liu HP, Li LH, et al: High frequency of epidermal growth factor receptor mutations with complex patterns in non–small cell lung cancers related to gefitinib responsiveness in Taiwan. Clin Cancer Res 10:8195-8203, 2004

11. Shigematsu H, Lin L, Takahashi T, et al: Clinical and biological features associated with epidermal growth factor receptor gene mutations in lung cancers. J Natl Cancer Inst 97:339-346, 2005

12. Marchetti A, Martella C, Felicioni L, et al: *EGFR* mutations in non–small-cell lung cancer: Analysis of a large series of cases and development of a rapid and sensitive method for diagnostic screening with potential implications on pharmacologic treatment. J Clin Oncol 23:857-865, 2005

13. Tokumo M, Toyooka S, Kiura K, et al: The relationship between epidermal growth factor receptor mutations and clinicopathologic features in non–small cell lung cancers. Clin Cancer Res 11:1167-1173, 2005

14. Noguchi M, Furuya S, Takeuchi T, et al: Modification formalin and methanol fixation methods for molecular biological and morphological analyses. Pathol Int 47:685-691, 1997

15. Hirsch FR, Varella-Garcia M, Bunn PA Jr, et al: Epidermal growth factor receptor in non-small-cell lung carcinomas: Correlation between gene copy number and protein expression and impact on prognosis. J Clin Oncol 21:3798-3807, 2003

16. Capuzzo F, Hirsch FR, Rossi E, et al: Epidermal growth factor receptor gene and protein and gefitinib sensitivity in non–small-cell lung cancer. J Natl Cancer Inst 97:643-655, 2005

17. Stephens P, Hunter C, Bignell G, et al: Lung cancer: Intragenic *ERBB2* kinase mutations in tumours. Nature 431:525-526, 2004

18. Shigematsu H, Takahashi T, Nomura M, et al: Somatic mutations of the *HER2* kinase domain in lung adenocarcinomas. Cancer Res 65: 1642-1646, 2005

19. Cappuzzo F, Magrini E, Ceresoli GL, et al: Akt phosphorylation and gefitinib efficacy in patients with advanced non-small-cell lung cancer. J Natl Cancer Inst 96:1133-1141, 2004

20. Han SW, Hwang PG, Chung DH, et al: Epidermal growth factor receptor (EGFR) downstream molecules as response predictive markers for gefitinib (Iressa, ZD1839) in chemotherapy resistant non-small-cell lung cancer. Int J Cancer 113:109-115, 2005

21. Franklin WA, Chansky K, Gumerlock PH, et al: Association between activation of ErbB pathway genes and survival following gefitinib treatment in advanced BAC (SWOG 0126). J Clin Oncol 22:618, 2004 (suppl; abstr 7015)

22. Emmert-Buck MR, Bonner RF, Smith PD, et al: Laser capture microdissection. Science 274:998-1001, 1996

23. Maeno G, Isobe T, Tokoro Y, et al: NAMIHEI: A novel algorithm for genomic polymorphism detection from DNA sequence. Genome Informatics 14:595-596, 2003

24. Ronaghi M: Pyrosequencing sheds light on DNA sequencing. Genome Res 11:3-11, 2001

25. Travis WD, Colby TV, Corrin B, et al: Histologic Typing of Tumors of Lung and Pleura: World Health Organization International Classification of Tumors (ed 3). New York, NY, Springer Verlag, 1999

26. Ebright M, Zakowski M, Martin J, et al: Clinical pattern and pathological stage but not histological features predict outcomes for bronchioloalveolar carcinoma (BAC). Ann Thorac Surg 74:1640-1646, 2002

27. Green S, Weiss GR: Southwest Oncology Group standard response criteria, endpoint definitions and toxicity criteria. Invest New Drugs 10:239-253, 1992

28. Kobayashi S, Boggon TJ, Dayaram T, et al: *EGFR* mutation and resistance of non-small-cell lung cancer to gefitinib. N Engl J Med 352:786-792, 2005

29. Pao W, Miller VA, Politi KA, et al: Acquired resistance of lung adenocarcinomas to gefitinib or erlotinib is associated with a second mutation in the EGFR kinase domain. PLoS Med 2:e73, 2005

30. Gorre ME, Mohammed M, Ellwood K, et al: Clinical resistance to STI-571 cancer therapy caused by BCR-ABL gene mutation or amplification. Science 293:876-880, 2001

31. Thatcher N, Chang A, Parikh P, et al: Results of a phase III placebo-controlled study (ISEL) of gefitinib (IRESSA) plus best supportive care (BSC) in patients with advanced non-small-cell lung cancer (NSCLC) who had received 1 or 2 prior chemotherapy regimens. Proc Am Assoc Cancer Res 46, 2005 (abstr LB-6)

for aggressive non-Hodgkin's lymphoma: a GELA study. Br J Haematol 2002;118:210-7.
3. Andre M, Mounier N, Leleu X, et al. Second cancers and late toxicities after treatment of aggressive non-Hodgkin lymphoma with the ACVBP regimen: a GELA cohort study on 2837 patients. Blood 2004;103:1222-8.
4. Bastion Y, Reyes F, Bosly A, et al. Possible toxicity with the association of G-CSF and bleomycin. Lancet 1994;343:1221-2.
5. Horning SJ, Weller E, Kim K, et al. Chemotherapy with or without radiotherapy in limited-stage diffuse aggressive non-Hodgkin's lymphoma: Eastern Cooperative Oncology Group study 1484. J Clin Oncol 2004;22:3032-8.

Phase 1 Clinical Trials in Oncology

TO THE EDITOR: Horstmann et al. (March 3 issue)[1] assume that a tumor response is of benefit to subjects in phase 1 oncology trials. This assumption is not valid. A complete or partial tumor response in a phase 1 trial is a surrogate end point, which for most agents has not been linked to a clinically meaningful outcome, such as improved survival.[2]

Informing subjects that they have a 10.6 percent chance of a tumor response is potentially misleading unless accompanied by an explicit discussion of clinical end points and whether any connection exists between a tumor response and clinical end points.[3] This discussion should include an explanation that a tumor response is not a cure or a life extender.

Kurzrock and Benjamin's editorial[4] serves only to increase the misrepresentation of phase 1 research.[5] It is important to know that phase 1 research is essential for the development of future treatments. But it is simply misleading to treat an improvement in the rate of tumor response as an increase in the likelihood of direct clinical benefit to subjects.

Barbra B. Rothschild, M.D.
Nancy M.P. King, J.D.

University of North Carolina at Chapel Hill
Chapel Hill, NC 27599
rothschild@unc.edu

1. Horstmann E, McCabe MS, Grochow L, et al. Risks and benefits of phase 1 oncology trials, 1991 through 2002. N Engl J Med 2005; 352:895-904.
2. Fleming TR, DeMets DL. Surrogate end points in clinical trials: are we being misled? Ann Intern Med 1996;125:605-13.
3. King NMP, Henderson GE, Churchill LR, et al. Consent forms and the therapeutic misconception: the example of gene transfer research. IRB 2005;27(1):1-8.
4. Kurzrock R, Benjamin RS. Risks and benefits of phase 1 oncology trials, revisited. N Engl J Med 2005;352:930-1.
5. Dresser R. The ubiquity and utility of the therapeutic misconception. Soc Philos Policy 2002;19(2):271-94.

TO THE EDITOR: The article by Horstmann et al. and the accompanying editorial indicate rates of clinical benefit higher than those reported in previous meta-analyses. Horng et al.,[1] in a critique of informed consent in phase 1 oncology trials, decried the frequent lack of an explicit statement that efficacy was not to be expected. However, in addition to evidence presented by Horstmann et al., recent phase 1 trials with established drugs have often resulted in high response rates. Among nine trials involving patients with refractory non–small-cell lung cancer that were presented at the meeting of the American Society of Clinical Oncology in May 2002, the reported response rate was 41 percent (range, 0 to 57 percent) in 150 patients, with one drug-related death recorded. Prior estimates of the risks and benefits of phase 1 oncology trials need updating, and insistence on not conveying therapeutic intent in the informed-consent process in all instances is misplaced.

Franco M. Muggia, M.D.

New York University Cancer Institute
New York, NY 10016
muggif01@med.nyu.edu

1. Horng S, Emanuel EJ, Wilfond B, Rackoff J, Martz K, Grady C. Descriptions of benefits and risks in consent forms for phase 1 oncology trials. N Engl J Med 2002;347:2134-40.

TO THE EDITOR: In their review of 460 phase 1 oncology trials sponsored by the Cancer Therapy Evaluation Program between 1991 and 2002, Horstmann et al. report that the overall toxicity-related death rate was 0.49 percent, which suggests that these trials are relatively safe, considering that virtually all participants have a deadly disease and have exhausted the conventional treatments.[1]

We analyzed the data from 363 trials of investigational new drugs, involving 12,395 adults with solid tumors, that were published between 1976 and

1993.[2] A total of 117 toxicity-related deaths (0.94 percent) and 33 early deaths from unknown causes (0.27 percent) were noted. In addition, 36 trials were excluded from the analysis because further clinical development of the drug was not recommended. We found that toxicity-related death occurred in 26 of 1039 patients in these trials (2.5 percent). Thus, the rate of death due to toxic events varies among phase 1 oncology trials and may be higher than suspected.

Ikuo Sekine, M.D., Ph.D.
Tomohide Tamura, M.D.
National Cancer Center Hospital
Tokyo 104-0045, Japan
isekine@ncc.go.jp

1. Kurzrock R, Benjamin RS. Risks and benefits of phase 1 oncology trials, revisited. N Engl J Med 2005;352:930-2.
2. Sekine I, Yamamoto N, Kunitoh H, et al. Relationship between objective responses in phase I trials and potential efficacy of nonspecific cytotoxic investigational new drugs. Ann Oncol 2002;13:1300-6.

TO THE EDITOR: Kurzrock and Benjamin argue that clinical benefit is an objective of phase 1 cancer trials, citing my article as an instance of an opposing "misconception."[1] The misconception is theirs, as is evident in authoritative definitions.[2,3] Moreover, in failing to distinguish between what phase 1 trials are specifically designed to measure (dose–toxicity profiles) and what is incidental to the design (e.g., the possibility of benefit), Kurzrock and Benjamin ignore the way in which the strictures of protocol constrain the goals of medicine. This misunderstanding, known as the "therapeutic misconception,"[4] reinforces the fiction that clinical research is an extension of clinical care, rather than a fundamentally distinct and sometimes contrary enterprise. Patients in early cohorts in these trials who receive, by design, what Kurzrock and Benjamin call "subtherapeutic" doses are not involved in a trial that aims to maximize their clinical benefit. Failure to see this as a conflict between the objectives of science and those of personal care is the reason the therapeutic misconception has been called "the most important threat to the validity of informed consent to research."[5]

Matthew J. Miller, M.D., M.P.H.
Harvard School of Public Health
Boston, MA 02115

1. Miller M. Phase 1 cancer trials: a crucible of competing priorities. Int Anesthesiol Clin 2001;139:13-33.
2. National Cancer Institute dictionary of cancer terms. (Accessed May 19, 2005, at http://www.cancer.gov/dictionary/db_alpha.aspx?expand=p#phase%201%20trial.)
3. Eisenhauer EA, O'Dwyer PJ, Christian M, Humphrey JS. Phase I clinical trial design in cancer drug development. J Clin Oncol 2000;18:684-92.
4. Appelbaum PS, Roth LH, Lidz CW, Benson P, Winslade W. False hopes and best data: consent to research and the therapeutic misconception. Hastings Cent Rep 1987;17:20-4.
5. Ethical and policy issues in international research: clinical trials in developing countries. Bethesda, Md.: National Bioethics Advisory Commission, 2001:48.

THE AUTHORS REPLY: The letters from Drs. Rothschild and King and from Dr. Muggia demonstrate the complexity of understanding "benefits" in the context of phase 1 oncology trials. As Drs. Rothschild and King suggest, tumor response, the most common measure of the effect of agents used for the treatment of cancer, is indeed a surrogate marker. Although tumor response does not necessarily correlate with clinical benefit, it is predictive of potential benefit, and there is evidence that tumor response is associated with symptom relief, improved quality of life, and increased survival.[1-4]

We agree that information provided to potential participants in phase 1 trials should be comprehensive, contextual, and clear about the uncertain or inconsistent relationship of possible tumor responses to clinically meaningful benefit.

Furthermore, it should be made clear that although some participants in phase 1 trials may benefit clinically, these trials are designed to evaluate safety, not therapeutic effect. There is a difference between the possibility of benefit from an intervention in a trial and the intent of the researchers when designing the trial. In this regard, we disagree with Dr. Muggia and maintain that consent forms should not describe the purpose or intent of phase 1 trials as therapeutic. Nonetheless, we recognize that although institutional review boards, bioethicists, and others might emphasize the intention of a trial, prospective patients may be more interested in possible benefits than in whether or not the trial is intended to be therapeutic. Our data demonstrate that sometimes there is therapeutic benefit, regardless of the intention of the research.

The statement by Drs. Sekine and Tamura that "the rate of death due to toxic events varies among phase 1 oncology trials" is consistent with the findings of our study. The data they cite emphasize two important realities that should be considered with

regard to response or toxicity rates in phase 1 trials: first, different subsets of data have strikingly different benefit and toxicity rates, and second, response and toxicity rates based on published data may be biased. Their data support the view that the details of a trial matter in interpreting the data on response and toxicity. Simply labeling a trial phase 1 is not sufficiently informative about risks and benefits; more specific details about the trial and the intervention are necessary.

Elizabeth Horstmann, B.A.
Ezekiel J. Emanuel, M.D., Ph.D.
Christine Grady, R.N., Ph.D.
National Institutes of Health
Bethesda, MD 20892-1156
cgrady@nih.gov

1. Lokich J. Tumor response and survival end points in clinical trials: a clinician's perspective. Am J Clin Oncol 2004;27:494-6.
2. Pazdur R. Response rates, survival, and chemotherapy trials. J Natl Cancer Inst 2000;92:1552-3.
3. Modi S, Panageas KS, Duck E, et al. Prospective exploratory analysis of the association between tumor response, quality of life, and expenditures among patients receiving paclitaxel monotherapy for refractory metastatic breast cancer. J Clin Oncol 2002;20:3665-73.
4. Geels P, Eisenhauer E, Bezjak A, Zee B, Day A. Palliative effect of chemotherapy: objective tumor response is associated with symptom improvement in patients with metastatic breast cancer. J Clin Oncol 2000;18:2395-405.

THE EDITORIALISTS REPLY: Rothschild and King's allegation that it is "misleading to treat an improvement in the rate of tumor response as an increase in the likelihood of direct clinical benefit to subjects" is at variance with our clinical experience and the oncology literature. Decades ago, Freireich et al.[1] established that improvement in survival in leukemia could be attributed directly to the duration of a response. A response to chemotherapy in randomized trials improved the quality of life despite significant side effects.[2] Differences in benefit between patients with and those without a response may be obscured, however, by an inadequate definition of a response. For example, patients with gastrointestinal stromal tumors who were treated with imatinib mesylate and who had stable disease according to the criteria of the Response Evaluation Criteria in Solid Tumors group derived a benefit that was indistinguishable from the benefit in those with a partial response.[3] Logic dictates that patients with good performance status and intact organ function — the eligibility criteria for most phase 1 studies — will not die of their cancer unless it progresses.

The perception that, in phase 1 studies, drugs are administered to patients solely to reveal drug toxicity is incorrect, since the objectives of phase 1 trials specifically include describing the response. Oncologists refer patients for phase 1 studies because they determine that participation in those studies offers their patients, whose disease has progressed after recognized therapies, their best chance of benefit. Thus, the primary concern of treating physicians and patients is efficacy. Miller's contention that the scientific restrictions of the protocols interfere with patient care is partially valid. For instance, some patients who might benefit are excluded from phase 1 trials by the eligibility criteria. Low initial doses and small dose increases, resulting from excessive caution about patient safety, can detract from benefit to patients. Nonetheless, as Horstmann et al. have demonstrated, phase 1 studies resulted in stable disease or better in up to 44.7 percent of patients, including those treated at the lower doses.

Increased time before the progression of cancer benefits patients unless the therapy has serious toxic effects. The worse "toxicity" is most often that due to progressive disease. We agree with Muggia, who demonstrates that recent phase 1 trials have higher response rates than previously reported and have extraordinarily low death rates. Although participants in any study should be informed that patients who have a response to therapy may not always benefit, it is misleading to tell patients that there is no clinical benefit from a response and that phase 1 trials have no therapeutic aim.

Razelle Kurzrock, M.D.
Robert S. Benjamin, M.D.
University of Texas M.D. Anderson Cancer Center
Houston, TX 77030

1. Freireich EJ, Gehan EA, Sulman D, Boggs DR, Frei E III. The effect of chemotherapy on acute leukemia in the human. J Chronic Dis 1961;14:593-608.
2. Coates A, Gebski V, Bishop JF, et al. Improving the quality of life during chemotherapy for advanced breast cancer: a comparison of intermittent and continuous treatment strategies. N Engl J Med 1987;317:1490-5.
3. Choi H, Charnsangavej C, Macapinlac HA, et al. Correlation of computerized tomography (CT) and positron emission tomography (PET) in patients with metastatic GIST treated at a single institution with imatinib mesylate. Prog Proc Am Soc Clin Oncol 2003; 22:819. abstract.

0090-9556/05/3305-630–636$20.00
DRUG METABOLISM AND DISPOSITION

DMD 33:630–636, 2005

Vol. 33, No. 5
3830/1198100
Printed in U.S.A.

FUNCTIONAL CHARACTERIZATION OF FIVE NOVEL CYP2C8 VARIANTS, G171S, R186X, R186G, K247R, AND K383N, FOUND IN A JAPANESE POPULATION

Hiroyuki Hichiya, Toshiko Tanaka-Kagawa, Akiko Soyama, Hideto Jinno, Satoru Koyano, Noriko Katori, Erika Matsushima, Shigehisa Uchiyama, Hiroshi Tokunaga, Hideo Kimura, Narihiro Minami, Masaaki Katoh, Kenji Sugai, Yu-ichi Goto, Tomohide Tamura, Noboru Yamamoto, Yuichiro Ohe, Hideo Kunitoh, Hiroshi Nokihara, Teruhiko Yoshida, Hironobu Minami, Nagahiro Saijo, Masanori Ando, Shogo Ozawa, Yoshiro Saito, and Jun-ichi Sawada

Project Team for Pharmacogenetics (H.H., A.S., H.J., S.K., N.K., S.O., Y.S., J.S.), Division of Environmental Chemistry (T.T.-K., H.J., E.M., S.U., H.T.), Division of Drugs (N.K.), Division of Pharmacology (S.O.), and Division of Biochemistry and Immunochemistry (Y.S., J.S.), National Institute of Health Sciences, Tokyo, Japan; National Institute of Neuroscience (H.Ki., N.M., Y.G.) and National Center Hospital for Mental, Nervous and Muscular Disorders (N.M, M.K., K.S.), National Center of Neurology and Psychiatry, Tokyo, Japan; Division of Internal Medicine (T.T., N.Y., Y.O., H.Ku., H.N.) and Genetics Division (T.Y.), National Cancer Center Research Institute, Tokyo, Japan; Division of Oncology/Hematology (H.M.) and Deputy Director (N.S.), National Cancer Center Hospital East, Chiba, Japan; and Faculty of Pharmacy, Musashino University, Tokyo, Japan (M.A.)

Received January 26, 2005; accepted February 15, 2005

ABSTRACT:

Cytochrome P450 2C8 is one of the primary enzymes responsible for the metabolism of a wide range of drugs such as paclitaxel, cerivastatin, and amiodarone. We have sequenced the *CYP2C8* gene from 201 Japanese subjects and found five novel nonsynonymous single nucleotide polymorphisms (SNPs): 511G>A (G171S), 556C>T (R186X; X represents the translational stop codon), 556C>G (R186G), 740A>G (K247R), and 1149G>T (K383N), with the allele frequency of 0.0025. The CYP2C8 variants were heterologously expressed in COS-1 cells and functionally characterized in terms of expression level, paclitaxel 6α-hydroxylase activity, and intracellular localization. The prematurely terminated R186X variant was undetectable by Western blotting and inactive toward paclitaxel 6α-hydroxylation. The G171S, K247R, and K383N variants exhibited properties similar to those of the wild-type CYP2C8. Paclitaxel 6α-hydroxylase activity of the R186G transfectant was only 10 to 20% that of wild-type CYP2C8. Furthermore, the R186G variant displayed a lower level of protein expression in comparison to the wild type, which was restored by the addition of a proteasome inhibitor (MG-132; Z-Leu-Leu-Leu-aldehyde). The reduced CO-difference spectral analysis using recombinant proteins from an insect cell/baculovirus system revealed that the R186G variant has a minor peak at 420 nm in addition to the characteristic Soret peak at 450 nm, suggesting the existence of improperly folded protein. These results indicate that the novel CYP2C8 SNPs, 556C>T (R186X) and 556C>G (R186G), could influence the metabolism of CYP2C8 substrates such as paclitaxel and cerivastatin.

Cytochrome P450 (P450) 2C8 plays an important role in the metabolism of xenobiotics and endogenous compounds in the human liver. CYP2C8 is also found in the extrahepatic tissues, including kidney, adrenal gland, brain, uterus, mammary gland, ovary, and duodenum (Klose et al., 1999). A wide range of drugs of clinical importance have been reported to be metabolized by CYP2C8. For instance, CYP2C8 catalyzes paclitaxel 6α-hydroxylation (Rahman et al., 1994), amiodarone *N*-deethylation (Ohyama et al., 2000), demethylation and hydroxylation of cerivastatin (Mück, 1998), repaglinide hydroxylation on the piperidine ring (Bidstrup et al., 2003), and chloroquine *N*-deethylation (Projean et al., 2003). Endogenous retinoids and arachidonic acid are also metabolized by CYP2C8 (Zeldin et al., 1996; Nadin and Murray 1999). Thus, genetic defects in the *CYP2C8* gene could lead to the altered metabolism/disposition of these medications.

The human *CYP2C8* gene has been assigned to chromosome 10q2e4.1 and is composed of nine exons (Inoue et al., 1994; Klose et al., 1999). To date, four allelic variants designated as *CYP2C8*2* to *CYP2C8*5* have been reported (for a classification of known CYP2C8 variant alleles, see http://www.imm.ki.se/CYPalleles/cyp2c8.htm). *CYP2C8*2* (I269F) is detected only in African-Americans, whereas *CYP2C8*3* (R139K and K399R) is found in both African-Americans and Caucasians (Dai et al., 2001). *CYP2C8*4* (I264M) has only been detected in Caucasians (Bahadur et al., 2002). As reported by Naka-

This study was supported in part by the Program for Promotion of Fundamental Studies in Health Sciences (MPJ-1, MPJ-2, and MPJ-6) of the Pharmaceuticals and Medical Devices Agency (PMDA) of Japan.

Hiroyuki Hichiya, Toshiko Tanaka-Kagawa, and Akiko Soyama contributed equally to this article.

Article, publication date, and citation information can be found at http://dmd.aspetjournals.org.

doi:10.1124/dmd.105.003830.

ABBREVIATIONS: P450, cytochrome P450; ECFP, enhanced cyan fluorescent protein; EYFP, enhanced yellow fluorescent protein; PCR, polymerase chain reaction; RT, reverse transcription; SNP, single nucleotide polymorphism; SRS, substrate recognition site; MG-132, Z-Leu-Leu-Leu-aldehyde.

jima et al. (2003), no coding-region SNPs in *CYP2C8* have been found in the Japanese population except for the *CYP2C8*5* allele (475delA) (Soyama et al., 2002), which causes a frame-shift leading to premature termination at residue 177. Recently, this allelic variant has been identified in a patient suffering from rhabdomyolysis after administration of cerivastatin (Ishikawa et al., 2004). Accordingly, we have searched for novel coding-region SNPs in the *CYP2C8* gene from the Japanese population.

In the present study, we report five novel nonsynonymous SNPs in the *CYP2C8* gene from the Japanese population. The wild-type and variant CYP2C8s were heterologously expressed in COS-1 cells and Sf9 cells and functionally characterized for their enzyme activity (paclitaxel 6α-hydroxylation), intracellular localization, proteasomal degradation, and reduced CO-difference spectra.

Materials and Methods

Chemicals. Paclitaxel and 6α-hydroxypaclitaxel were obtained from BD Gentest (Woburn, MA). 7,13-Diacetyl baccatin III was purchased from Alexis Biochemicals (San Diego, CA). Emulgen 911 was a generous gift from KAO (Tokyo, Japan).

Preparation of Human Genomic DNA Samples and Sequencing of *CYP2C8* Gene. All of the 201 subjects in this study were Japanese cancer or epileptic patients. The ethical review boards of the National Cancer Center, the National Center of Neurology and Psychiatry, and the National Institute of Health Sciences approved this study. Written informed consent was obtained from all participating subjects. DNA extraction from blood leukocytes, PCR amplification of CYP2C8 exons, and DNA sequencing of each fragment were carried out as described previously (Soyama et al., 2001).

Construction of Plasmids. Construction of the wild-type CYP2C8 expression plasmid (pCR3.1/CYP2C8/WT) was described previously (Soyama et al., 2001). Mutations (511G>A, 556C>T, 556C>G, 740A>G, and 1149G>T) were introduced into the pCR3.1/CYP2C8/WT using a QuikChange multi site-directed mutagenesis kit (Stratagene, La Jolla, CA) with the following 5′-phosphorylated primers: 5′-TCCCACTTTCATCCTG**A**GCTGTGCTCCC-TGCAA-3′ for 511G>A, 5′-GCTCCGTTGTTTTCCAGAAA**T**GATTTGAT-TATAAAGATC-3′ for 556C>T, 5′-GCTCCGTTGTTTTCCAGAAA**G**GAT-TTGATTATAAAGATC-3′ for 556C>G, 5′-CGAAGTTACATTAGGGAG-A**G**AGTAAAAGAACACCAAGC-3′ for 740A>G, and 5′-ACTACCTCAT-CCCCAA**T**GGCACAACCATAATGG-3′ for 1149G>T. The bases exchanged are boldface and underlined. To ensure that no errors had been introduced during the amplification process, all the plasmid constructs were verified by DNA sequencing of both strands.

For the construction of C-terminal ECFP-tagged CYP2C8 expression plasmids, CYP2C8 cDNAs were reamplified by PCR using each cDNA in pCR3.1 as a template with the following primers: 5′- CACCATGGAACCTTTTGT-GGTC-3′ and 5′-GACAGGGATGAAGCAGATCTGG-3′. The underlined sequence was introduced for directional TOPO cloning. The latter reverse primer lacks the stop codon in the native CYP2C8 cDNA. The resulting CYP2C8 cDNAs (designated CYP2C8ΔTGA) were first cloned into pENTR/D-TOPO vectors (Invitrogen, Carlsbad, CA), and then subcloned into pDONR207 vectors (Invitrogen). Conversion of the pECFP-N1 vector (BD Biosciences Clontech, Palo Alto, CA) to a Gateway-compatible destination vector was carried out using the Gateway Vector Conversion System (Invitrogen) according to the manufacturer's instructions. Specifically, the pECFP-N1 vector was digested with XhoI and BamHI, blunted with T4 DNA polymerase, and then ligated with Gateway reading-frame cassette B fragment. The resulting pECFP vector was designated pECFP-DEST. Each CYP2C8ΔTGA cDNA in pDONR207 was subcloned into pECFP-DEST vector by the Gateway LR reaction.

Heterologous Expression of CYP2C8s in COS-1 Cells. Transfection of COS-1 cells with pCR3.1/CYP2C8 vectors were essentially the same as described previously (Jinno et al., 2003a). Mock transfections were carried out using pCR3.1 vector without an insert. Forty-eight hours after transfection, microsomes from COS-1 cells were prepared by sequential centrifugation according to the standard procedure described by Ekins et al. (1999). Microsomes were then suspended in 100 mM potassium phosphate buffer (pH 7.4) containing 10% glycerol and stored at −80°C until use.

In the experiments on the proteasomal degradation of CYP2C8, COS-1 cells were treated with 10 μM MG-132 (Sigma-Aldrich, St. Louis, MO) after 24 h post-transfection. The cells were incubated for another 8 h and harvested in ice-cold buffered sucrose. The whole-cell lysates were prepared by sonication and subjected to Western blot analysis.

Determination of CYP2C8 mRNA by Real-Time RT-PCR. Total cellular RNA was isolated from the COS-1 cells using the RNeasy Mini kit (QIAGEN, Tokyo, Japan) in combination with the RNase-free DNase treatment to minimize plasmid DNA contamination of samples. First-strand cDNA was prepared from 1 μg of total cellular RNA using a High-Capacity cDNA Archive kit (Applied Biosystems, Foster City, CA) with random primers. Real-time PCR assays were performed on an ABI7000 using TaqMan gene expression assays for CYP2C8 (Hs00426387_m1; Applied Biosystems) according to the manufacturer's recommendations. The relative abundance of mRNA levels was determined from calibration curves generated from a serial dilution of the pooled cDNA from COS-1 cells expressing wild-type CYP2C8. Samples without reverse transcriptase were routinely included in the RT-PCR reactions to measure the possible interference of the contaminated DNA, which was usually less than 1% of the mRNA-derived amplification. Transcripts of β-actin were quantified as internal controls using TaqMan β-actin Control Reagent (Applied Biosystems), and CYP2C8 mRNA levels were normalized on the basis of their β-actin content.

Intracellular Localization of ECFP-Tagged CYP2C8 in COS-1 Cells. COS-1 cells, plated in a six-well culture plate at a density of 4×10^4 cells/cm^2, were transfected with 4 μg of pECFP-N1/CYP2C8s or pEYFP-ER (BD Biosciences Clontech), an endoplasmic reticulum localization vector, using LipofectAMINE 2000 reagent. Twenty-four hours after transfection, fluorescence microscopic observation of the ECFP-tagged CYP2C8s and EYFP protein was performed using an Eclips TE2000 inverted microscope (Nikon, Tokyo, Japan) equipped with Cyan GFP V2 and Yellow GFP BP filters (Chroma Technology Corp., Brattleboro, VT). Images were captured using a cooled charge-coupled device camera (ORCA-ER; Hamamatsu Photonics, Shizuoka, Japan).

Heterologous Expression of CYP2C8s in *Spodoptera frugiperta* (Sf9) Cells. The intact wild-type and R186G variant CYP2C8 cDNAs were cloned into pENTR/D-TOPO vectors using a strategy similar to that for CYP2C8ΔTGA cDNAs except that a different reverse primer was used for the amplification: 5′-TCAGACAGGGATGAAGCAGATC-3′. Baculovirus construction and protein expression in Sf9 cells were performed according to the BaculoDirect Baculovirus Expression System protocol from Invitrogen. Briefly, Sf9 cells were directly transfected with the recombinant baculovirus DNA, which was generated by the LR reaction between the entry clone (pENTR/CYP2C8s) and the BaculoDirect linear DNA. The cells were selected with ganciclovir for 5 days, and the resulting viral stock was amplified twice by infecting the Sf9 cells. Finally, a high-titer viral stock (>10^8 pfu/ml) was obtained.

Sf9 cells were infected with BaculoDirect/CYP2C8 with a multiplicity of infection of 2. After 24 h postinfection, δ-aminolevulinic acid (0.1 mM) and ferric citrate (0.1 mM) were added to the Sf9 cells to compensate for a deficiency in heme biosynthesis (Schwarz et al., 2001). The cells were harvested 72 h postinfection. Cells were lysed in 0.1 M potassium phosphate buffer, pH 7.4, containing 20% glycerol, 0.1 mM EDTA, 0.1 mM dithiothreitol, and 0.4% Emulgen 911 (KAO) by incubation for 30 min on ice with occasional agitation. After centrifugation, the resulting whole-cell lysate was diluted to a total protein concentration of 10 mg/ml. The reduced CO-difference spectra were recorded as described by Gonzalez et al. (1991) using an UV-visible spectrophotometer (Shimadzu UV-2400PC; Shimadzu, Kyoto, Japan).

Western Blotting. Microsomal fractions (30 μg/lane), or whole-cell lysates (10 μg/lane) from COS-1 cells or Sf9 cells (0.5 μg/lane) were separated by 10% sodium dodecyl sulfate-polyacrylamide gel electrophoresis and electroblotted onto a polyvinylidene difluoride membrane (ATTO, Tokyo, Japan). The membrane was incubated with rabbit anti-human CYP2C8 antibody (diluted at 1:2000; Research Diagnostics, Flanders, NJ) as the primary antibody and then with horseradish peroxidase-conjugated donkey anti-rabbit Ig (1:2000; Amersham Biosciences Inc., Piscataway, NJ) as the secondary anti-

body. Immunoreactive proteins were visualized with chemifluorescence (ECL-Plus reagents; Amersham Biosciences), and the band densities were quantified using the Typhoon 9400 Variable Mode Imager and ImageQuant analysis software. A commercially available human CYP2C8 protein expressed in insect cells (Supersomes; BD Gentest, Woburn, MA) was used as a calibration standard. To confirm that the samples were evenly loaded, the blot derived from the COS-1 cells was subsequently stripped and reprobed with a polyclonal anti-calnexin antibody (diluted at 1:100,000; StressGen Biotechnologies, San Diego, CA) as described previously (Jinno et al., 2003a).

Enzyme Assay. The paclitaxel 6α-hydroxylase activities of wild-type and variant CYP2C8s were assayed as described previously (Soyama et al., 2001) at eight different substrate concentrations between 0.5 and 20 μM. The limit of quantitation for 6α-hydroxypaclitaxel was 30 pmol/ml, which corresponded to the enzyme activity of 1.3 pmol/min/mg protein. Kinetic parameters were calculated with Prism 4.0 (GraphPad Software Inc., San Diego, CA) using nonlinear regression of the Michaelis-Menten equation.

Data Analysis. Statistical comparisons were performed by one-way analysis of variance with Dunnett's post hoc test using Prism 4.0. Differences were considered to be statistically significant when the p value was <0.01.

Results

Novel Genetic Variations of Human CYP2C8. From the sequence analysis of 201 Japanese subjects, five novel nonsynonymous SNPs were identified in the coding region of the *CYP2C8* gene. These results were confirmed by repeating the PCR on genomic DNA and sequencing the newly amplified products. The novel SNPs include 511G>A (exon 4, resulting in the amino acid substitution of G171S), 556C>T (exon 4, R186X; X represents the translational stop codon), 556C>G (exon 4, R186G), 740A>G (exon 5, K247R), and 1149G>T (exon 7, K383N): these alleles have been designated *CYP2C8*6*, **7*, **8*, **9*, and **10*, respectively, by the Human CYP Allele Nomenclature Committee (http://www.imm.ki.se/CYPalleles/). Each SNP was found in a distinct subject as a heterozygote with an allele frequency of 0.0025. *CYP2C8*5* allele (475delA) was not found in the present study. Figure 1 depicts the representative electropherograms of the SNPs.

Expression of the Wild-Type and Variant CYP2C8s in COS-1 Cells. To functionally characterize the nonsynonymous CYP2C8 variants, the wild-type and variant CYP2C8 proteins were transiently expressed in COS-1 cells. As shown in Fig. 2, A and B, the protein expression levels of the R186G variant was only ~40% that of the wild-type ($p < 0.01$ by one-way analysis of variance and Dunnett's test), whereas those of G171S, K247R, and K383N were slightly reduced (not statistically significant). These differences in the levels of recombinant protein within the cell were reproducible in three independent transfection experiments. R186X variant protein was undetectable even as proteolytic fragment bands under this experimental condition (data not shown).

CYP2C8 mRNA expression levels in the transfected COS-1 cells were measured by real-time RT-PCR. As shown in Fig. 2C, no significant differences were detected in the level of mRNA among the four CYP2C8 variants, suggesting that the observed disparity in the level of CYP2C8 protein was not due to variation in the transfection/transcription efficiency of the plasmid constructs.

Paclitaxel 6α-Hydroxylase Activities of the Wild-Type and Variant CYP2C8s Expressed in COS-1 Cells. The CYP2C8 variants were functionally characterized for the hydroxylase activity toward a representative CYP2C8 substrate, paclitaxel. In Fig. 3, paclitaxel 6α-hydroxylase activities of the CYP2C8s were expressed on the basis of microsomal protein (Fig. 3A) or CYP2C8 content (Fig. 3B). Except for R186X and R186G, enzyme activities of the variants were almost comparable to that of the wild type, regardless of the low (0.5 μM) and high (20 μM) substrate concentrations. In contrast, the R186G variant showed a markedly lower turnover rate; no 6α-hydroxylated metabolite was detected at the low substrate concentration, and the metabolite generated at the high concentration was approximately 20% of that of wild-type on the basis of pmol/min/pmol CYP2C8 ($p < 0.01$). For the R186X variant, no enzyme activity was observed even at the high substrate concentration of 20 μM, indicating that the residual activity was less than 2% of the wild-type.

We attempted to determine the kinetic parameters for the paclitaxel 6α-hydroxylase reaction of the CYP2C8 variants. The representative nonlinear regression curves of the Michaelis-Menten kinetics are shown in Fig. 4. Kinetic parameters for the R186G variant could not be accurately established using high performance liquid chromatography analysis due to the low turnover rates. As summarized in Table 1, the apparent K_m and V_{max} values of wild-type were 7.08 ± 0.30 μM, 87.4 ± 8.6 pmol/min/mg protein, and 32.4 ± 3.4 pmol/min/pmol CYP2C8, respectively. The K_m value was almost comparable to those previously reported for the yeast-expressed CYP2C8 (10 μM) and human liver microsomes (12–15 μM) (Cresteil et al., 2002; Melet et al., 2004; Taniguchi et al., 2005). No statistically significant difference was observed in the K_m value of wild-type and each variant.

Intracellular Localization of CYP2C8 Proteins in COS-1 Cells. In eukaryotes, P450 enzymes are localized either on the outer side of the endoplasmic reticulum or on the inner membrane of mitochondria. To test whether the lower than expected level of R186G variant in the microsomal fraction could be the result of altered intracellular location, we tested the localization of CYP2C8 proteins using C-terminal ECFP-tagged CYP2C8s. pEYFP-ER was included as a control to demonstrate the representative localization in endoplasmic reticulum. As shown in Fig. 5, no apparent difference was recorded in the intracellular localization of each CYP2C8, which was similar to the localization of the microsome-oriented EYFP protein. These results indicate that intracellular localization does not account for the decreased R186G level.

Proteasomal Degradation of R186G Variant. To further clarify the molecular mechanisms underlying the decreased expression of R186G, involvement of the proteasomal degradation pathway was investigated by using a proteasome inhibitor, MG-132. COS-1 cells expressing either wild-type or R186G CYP2C8 were treated with MG-132 (10 μM) for 8 h. Upon treatment of the cells with MG-132, the decrease in the expression level of R186G variant was restored to a level almost comparable with that of wild-type CYP2C8 (Fig. 6). This finding suggests that the enhanced proteasomal degradation of the R186G variant could explain the observed decrease in the level of protein.

Spectral Analysis of Wild-Type CYP2C8 and R186G Variant. The reduced CO-difference spectral analysis was carried out using recombinant wild-type CYP2C8 and R186G variant proteins heterologously expressed in Sf9 cells. The relative expression level of the R186G variant protein was approximately 70% of the wild-type, as shown in Fig. 7. The reduced CO-difference spectrum of wild-type CYP2C8 comprised a single Soret peak at 450 nm. In contrast, an equivalent spectrum of the R186G variant had a minor peak at 420 nm in addition to a major peak at 450 nm. It is likely that the 420-nm peak corresponds to an inactive form of the variant. These results, together with those on the proteasomal degradation, suggest that a proportion of the R186G variant might be improperly folded or unstable.

Discussion

To date, several SNPs have been reported in the human *CYP2C8* gene. Dai et al. (2001) identified two *CYP2C8* alleles designated as *CYP2C8*2* (805A>T, I269F) and *CYP2C8*3* (416G>A and 1196A>G, R139K and K399R). *CYP2C8*2* was only found in African-Americans (allele fre-

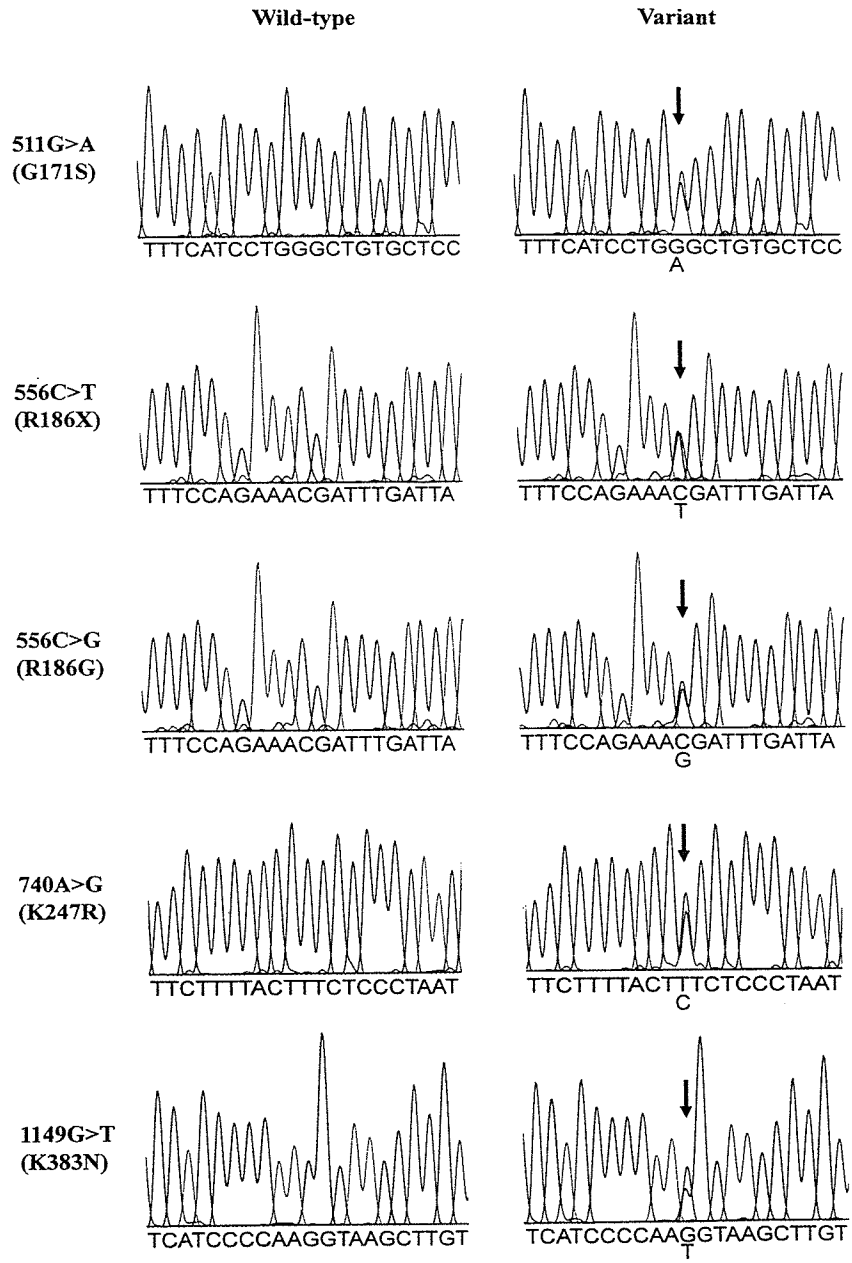

FIG. 1. Electropherograms of the novel nonsynonymous SNPs of *CYP2C8* gene. Arrows indicate the positions of the nucleotide changes. Note that electropherograms of the sense-strand are shown except for the 740A>G (K247R) variant.

quency, 0.18) and *CYP2C8*3* primarily in Caucasians (allele frequency, 0.13), whereas neither allele was found in Asians. Bahadur et al. (2002) reported the *CYP2C8*4* allele (792C>G, I264M) at an allele frequency of 0.075 and a rare SNP, 1169T>C (L390S). In addition, we discovered a *CYP2C8*5* allele (475delA, resulting in an early stop codon at residue 177) in a Japanese subject and a 1210C>G substitution (P404A) in an established cell line derived from a Japanese individual (Soyama et al., 2001, 2002). Among these allelic variants, CYP2C8.3 (R139K/K399R) exhibits reduced paclitaxel 6α-hydroxylase activity (Dai et al., 2001; Bahadur et al., 2002), whereas CYP2C8.2 has a 2-fold higher K_m and a 2-fold lower intrinsic clearance, or V_{max}/K_m value, compared with CYP2C8.1 (Dai et al., 2001). A similar decrease in the intrinsic clearance was observed for P404A, which was mainly caused by the reduced protein expression level (Soyama et al., 2001). Recently, Nakajima et al. (2003) have screened more than 200 Japanese individuals for the known SNPs in the coding region of *CYP2C8*. From this screen they found only a heterozygous *CYP2C8*5* allele at a frequency of 0.0025, indicating that the coding-region SNPs in *CYP2C8* are relatively rare in Japanese. The present study supports these findings, except that we identified five novel nonsynonymous substitutions; 511G>A (G171S), 556C>T (R186X), 556C>G (R186G), 740A>G (K247R) and 1149G>T (K383N). These SNPs were found in distinct subjects as heterozygotes. The allele frequency of each SNP was 0.0025.

To characterize the functional alteration(s) of the novel CYP2C8 variants, their paclitaxel 6α-hydroxylase activities were first determined using the recombinant proteins heterologously expressed in COS-1 cells. The enzyme activity of the R186X and R186G variants were undetectable (R186X, data not shown) or almost one tenth of the wild-type (R186G, Fig. 2). The null enzyme activity of the R186X variant was fully expected given that it lacks approximately 60% of the C-terminal region, including the heme-binding site. However, R186G exhibited a markedly reduced paclitaxel 6α-hydroxylase ac-

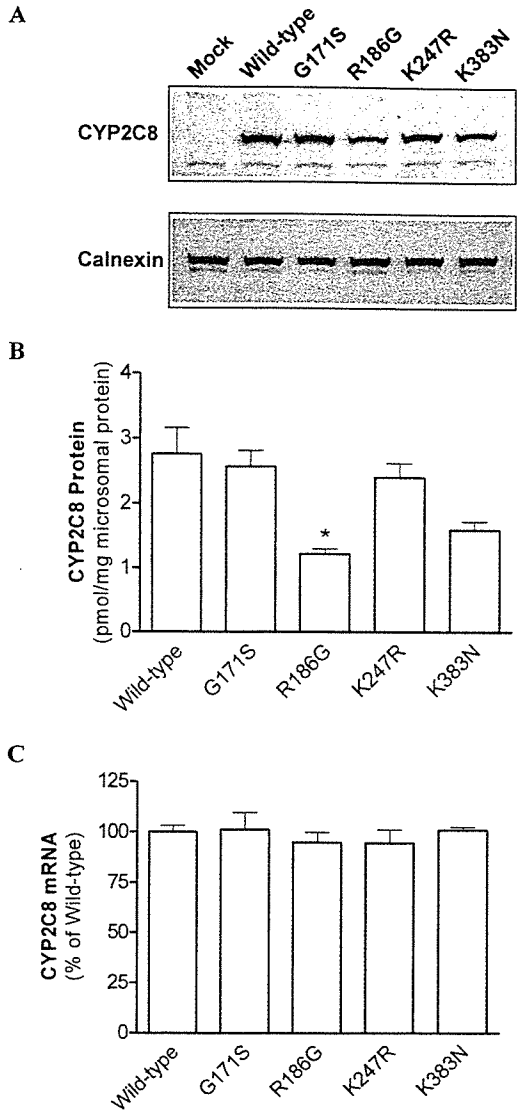

FIG. 2. Expression of wild-type and variant CYP2C8s in COS-1 cells. A, aliquots (30 μg) of the pooled microsomes from three independent preparations were subjected to Western blot analysis. Wild-type and variant CYP2C8s were detected with rabbit anti-human CYP2C8 antiserum (diluted at 1:2000) as described under *Materials and Methods*. To confirm that the samples were evenly loaded, the blot was subsequently stripped and reprobed with a polyclonal anti-calnexin antibody (diluted at 1:100,000). R186X variant protein was undetectable under this experimental condition (data not shown). B, the stained CYP2C8 bands of each Western blot from three independent preparations were quantified using the ImageQuant analysis software. The expression levels of CYP2C8 proteins are shown. C, CYP2C8 mRNA in the total cellular RNA samples was quantified using TaqMan RT-PCR. Each sample was normalized on the basis of the β-actin content and expressed as a percentage of wild type. Each bar represents the mean ± S.E.M. of three independent preparations. ⋆, significantly different from that of wild-type CYP2C8 at the level of $p < 0.01$.

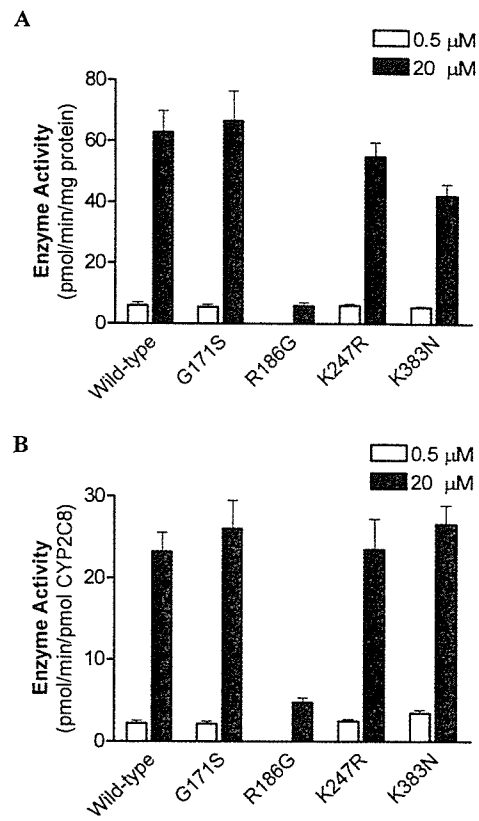

FIG. 3. Paclitaxel 6α-hydroxylase activities of wild-type and variant CYP2C8s. The substrate concentrations used were 0.5 and 20 μM. Enzyme activities were expressed in terms of pmol/min/mg protein (A) and pmol/min/pmol CYP2C8 (B). For the R186X variant, no enzyme activity was observed, even at the high substrate concentration, 20 μM (data not shown). Each bar represents the mean ± S.E.M. of three independent preparations.

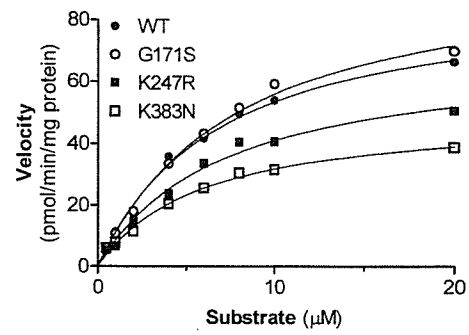

FIG. 4. Representative Michaelis-Menten kinetics for paclitaxel 6α-hydroxylation by recombinant wild-type and variant CYP2C8s. The solid line indicates fitting of data to the Michaelis-Menten equation by nonlinear regression.

tivity despite an intact heme-binding site and substrate recognition sites (SRSs) (Gotoh, 1992). Furthermore, the lower than expected level of R186G protein was reproducibly observed without any significant reduction in the level of corresponding mRNA (Fig. 2). No difference in the intracellular distribution of the R186G variant could be detected (Fig. 5). These results suggest that the R186G variant is less stable and/or more rapidly degraded than the wild-type protein in the heterologous expression system. Recent findings on the degradation of the ER-resident proteins including some P450 isoforms revealed a significant contribution from the ubiquitin-proteasome pathway (Correia, 2003; Bandiera et al., 2005). We examined the effect of a proteasome inhibitor, MG-132, on the expression level of R186G variant in COS-1 cells. MG-132 treatment restored the expression level of R186G to a level comparable to that of wild-type (Fig. 6). This clearly indicates that the decreased level of R186G protein compared with wild-type is the result of enhanced proteasome-mediated degradation.

Reduced enzyme activity and extensive degradation of the R186G variant might be indicative of a structural defect of CYP2C8 apoprotein. Although the transient expression system in COS-1 cells has been successfully applied to the functional analysis of P450 variants including CYP2B6, CYP2E1, and CYP1B1 (Hanioka et al., 2003; Jinno et al., 2003b; Bandiera et al., 2005), the primary drawback of this heterologous system is insufficient levels of recombinant proteins

TABLE 1

Kinetic parameters for paclitaxel 6α-hydroxylase activities of wild-type and variant CYP2C8

Each value represents the mean ± S.E.M. of three independent transfection experiments.

CYP2C8	K_m	V_{max}		V_{max}/K_m	
		pmol/min/mg protein	pmol/min/pmol P450	μl/min/mg protein	μl/min/pmol P450
	μM				
Wild-type	7.08 ± 0.30	87.4 ± 8.6	32.4 ± 3.4	12.5 ± 1.7	4.60 ± 0.54
G171S	7.80 ± 0.13	96.4 ± 13.7	37.7 ± 4.9	12.4 ± 1.9	4.85 ± 0.70
K247R	6.45 ± 0.83	76.1 ± 8.5	32.7 ± 6.1	11.9 ± 1.2	5.04 ± 0.51
K383N	6.44 ± 0.26	57.6 ± 5.6	36.1 ± 2.9	8.97 ± 0.95	5.66 ± 0.63

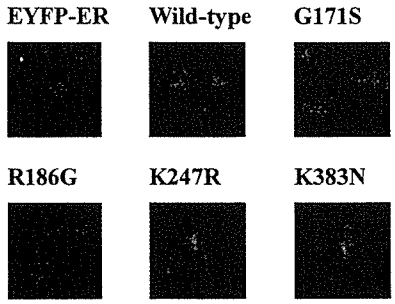

FIG. 5. Intracellular localization of CYP2C8 proteins in COS-1 cells. COS-1 cells, plated in a six-well culture plate at a density of 4×10^4 cells/cm^2, were transfected with 4 μg of pECFP-N1/CYP2C8s or pEYFP-ER. Twenty-four hours after transfection, fluorescence microscopic observation of the ECFP-tagged CYP2C8s and EYFP protein was performed as described under *Materials and Methods*.

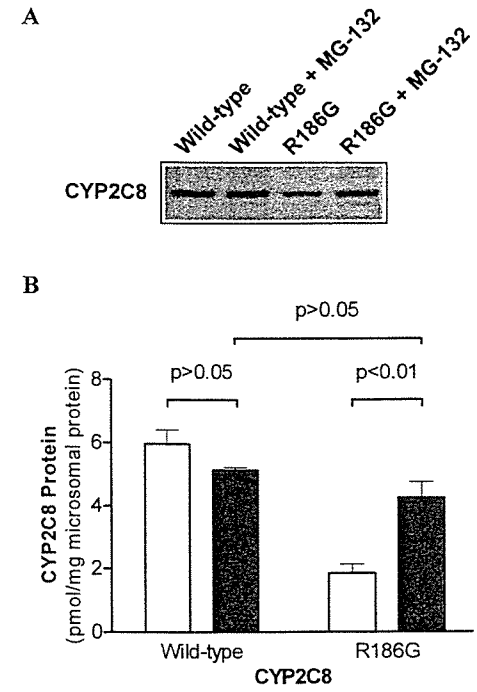

FIG. 6. Proteasomal degradation of the R186G variant CYP2C8. COS-1 cells were transfected with pCR3.1/CYP2C8 vectors (wild-type and R186G). After 24 h, the cells were treated with 10 μM MG-132 or vehicle (dimethyl sulfoxide) alone for another 8 h and then harvested in ice-cold buffered sucrose. The whole-cell lysates were prepared by sonication and subjected to Western blot analysis. A, aliquots (10 μg) of the pooled whole-cell lysates from three independent preparations were subjected to Western blotting with antibody against CYP2C8. B, the stained CYP2C8 bands of each Western blot were quantified using the ImageQuant analysis software. Open bars and closed bars indicate the CYP2C8 protein levels of the untreated and MG-132-treated cells, respectively. Each bar represents the mean ± S.E.M. of three independent preparations.

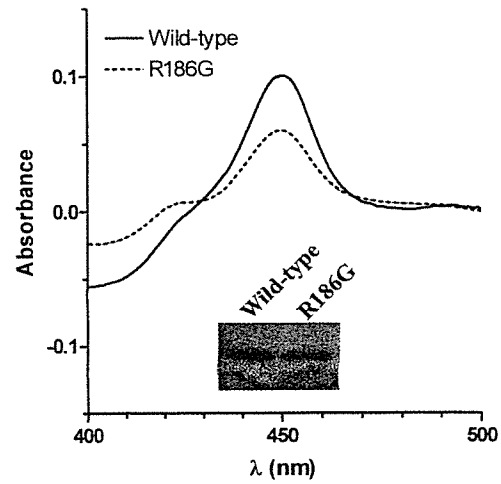

FIG. 7. Reduced CO-difference spectra of wild-type and R186G variant CYP2C8. The reduced CO-difference spectral analysis was carried out using recombinant wild-type CYP2C8 and R186G variant proteins heterologously expressed in Sf9 cells as described under *Materials and Methods*. Western blotting was performed using the whole-cell lysates from Sf9 cells (0.5 μg of protein/lane).

compared with the bacterial and baculovirus-mediated systems for structural analyses. Therefore, the wild type and R186G variant were further studied using insect cells/baculovirus system. The UV-visible spectrum of the R186G variant shows a minor peak at 420 nm in addition to the characteristic Soret peak at 450 nm (Fig. 7), indicating improper protein folding and/or incorporation of the heme group into the apoenzyme as reported by Imaoka et al. (1993) and Iwasaki et al. (1993). Taken together, these results suggest that the R186G substitution causes the formation of incorrectly folded enzyme, which is readily degraded by a proteasome-dependent mechanism.

The amino acid residue R186 is well conserved among the majority of the CYP2 subfamily enzymes including CYP2C9 and CYP2C19. The X-ray crystal structure of CYP2C8 shows that R186 is located in the loop between helices E and F (Schoch et al., 2004; Protein Data Bank, 1PQ2). To date, several functionally significant regions and residues in the P450s have been identified based on homology modeling and site-directed mutagenesis studies. For instance, the proline-rich motif (PPGPXPXPXXGN motif) in the N-terminal region of P450s plays a significant role in the proper assembly of the native enzyme (Kemper, 2004). In addition, Kerdpin et al. (2004) have reported that SRS1 and SRS5 of CYP2C8 are important for paclitaxel binding, and that S114 in SRS1 is especially critical for the interaction with the substrate. However, the R186 residue is not located in the proline-rich region or in the SRS regions. The R186G substitution in the E-F loop may influence the conformation or flexibility of the helices in the F-G region, which forms a lid to the active site and dimerization interface, causing a loss in enzyme activity (Schoch et al., 2004).

In summary, we identified five novel nonsynonymous SNPs from screening 201 Japanese subjects: 511G>A (G171S), 556C>T (R186X), 556C>G (R186G), 740A>G (K247R), and 1149G>T (K383N). Functional analyses of these CYP2C8 variants revealed that R186X has no detectable enzyme activity. The R186G variant showed a much reduced enzymatic activity in comparison to the wild-type enzyme. Although the allele frequencies of both these variants were rather low, it would be of clinical significance to evaluate the influence of these CYP2C8 variant alleles on the pharmacokinetics/pharmacodynamics of drugs such as paclitaxel and cerivastatin.

Acknowledgments. We thank Chie Knudsen for generous support.

References

Bahadur N, Leathart JBS, Mutch E, Steimel-Crespi D, Dunn SA, Gilissen R, Houdt JV, Hendrickx J, Mannens G, and Bohets H (2002) CYP2C8 polymorphisms in Caucasian and their relationship with paclitaxel 6α-hydroxylase activity in human liver microsomes. *Biochem Pharmacol* **64**:1579–1589.

Bandiera S, Weidlich S, Harth V, Broede P, Ko Y, and Friedberg T (2005) Proteasomal degradation of human CYP1B1: effect of the Asn453Ser polymorphism on the post-translational regulation of CYP1B1 expression. *Mol Pharmacol* **67**:435–443.

Bidstrup TB, Bjornsdottir I, Sidelmann UG, Thomsen MS, and Hansen KT (2003) CYP2C8 and CYP3A4 are the principal enzymes involved in the human in vitro biotransformation of the insulin secretagogue repaglinide. *Br J Clin Pharmacol* **56**:305–314.

Correia MA (2003) Hepatic cytochrome P450 degradation: mechanistic diversity of the cellular sanitation brigade. *Drug Metab Rev* **35**:107–143.

Cresteil T, Monsarrat B, Dubois J, Sonnier M, Alvinerie P, and Gueritte F (2002) Regioselective metabolism of taxoids by human CYP3A4 and 2C8: structure-activity relationship. *Drug Metab Dispos* **30**:438–445.

Dai D, Zeldin DC, Blaisdell JA, Chanas B, Coulter SJ, Ghanayem BI, and Goldstein JA (2001) Polymorphisms in human CYP2C8 decrease metabolism of the anticancer drug paclitaxel and arachidonic acid. *Pharmacogenetics* **11**:597–607.

Ekins S, Maenpaa J, and Wrighton SA (1999) In vitro metabolism: subcellular fractions, in *Handbook of Drug Metabolism* (Woolf TE ed) pp 363–399, Marcel Dekker, New York.

Gonzalez FJ, Kimura S, Tamura S, and Gelboin HV (1991) Expression of mammalian cytochrome P450 using baculovirus. *Methods Enzymol* **206**:93–99.

Gotoh O (1992) Substrate recognition sites in cytochrome P450 family 2 (CYP2) proteins inferred from comparative analyses of amino acid and coding nucleotide sequences. *J Biol Chem* **267**:83–90.

Hanioka N, Tanaka-Kagawa T, Miyata Y, Matsushima E, Makino Y, Ohno A, Yoda R, Jinno H, and Ando M (2003) Functional characterization of three human cytochrome p450 2E1 variants with amino acid substitutions. *Xenobiotica* **33**:575–586.

Imaoka S, Ogawa H, Kimura S, and Gonzalez FJ (1993) Complete cDNA sequence and cDNA-directed expression of CYP4A11, a fatty acid omega-hydroxylase expressed in human kidney. *DNA Cell Biol* **12**:893–899.

Inoue K, Inazawa J, Suzuki Y, Shimada T, Yamazaki H, Guengerich FP, and Abe T (1994) Fluorescence in situ hybridization analysis of chromosomal localization of three human cytochrome P450 2C genes (CYP2C8, 2C9 and 2C10) at 10q24.1. *Jpn J Hum Genet* **39**:337–343.

Ishikawa C, Ozaki H, Nakajima T, Ishii T, Kanai S, Anjo S, Shirai K, and Inoue I (2004) A frameshift variant of CYP2C8 was identified in a patient who suffered from rhabdomyolysis after administration of cerivastatin. *J Hum Genet* **49**:582–585.

Iwasaki M, Lindberg RL, Juvonen RO, and Negishi M (1993) Site-directed mutagenesis of mouse steroid 7 alpha-hydroxylase (cytochrome P-450(7) alpha): role of residue-209 in determining steroid-cytochrome P-450 interaction. *Biochem J* **291**:569–573.

Jinno H, Tanaka-Kagawa T, Hanioka N, Saeki M, Ishida S, Nishimura T, Ando M, Saito Y, Ozawa S, and Sawada J (2003a) Glucuronidation of 7-ethyl-10-hydroxycamptothecin (SN-38), an active metabolite of irinotecan (CPT-11), by human UGT1A1 variants, G71R, P229Q, and Y486D. *Drug Metab Dispos* **31**:108–113.

Jinno H, Tanaka-Kagawa T, Ohno A, Makino Y, Matsushima E, Hanioka N, and Ando M (2003b) Functional characterization of cytochrome P450 2B6 allelic variants. *Drug Metab Dispos* **31**:398–403.

Kemper B (2004) Structural basis for the role in protein folding of conserved proline-rich regions in cytochromes P450. *Toxicol Appl Pharmacol* **199**:305–315.

Kerdpin O, Elliot DJ, Boye SL, Birkett DJ, Yoovathaworn K, and Miners JO (2004) Differential contribution of active site residues in substrate recognition sites 1 and 5 to cytochrome P450 2C8 substrate selectivity and regioselectivity. *Biochemistry* **43**:7834–7842.

Klose TS, Blaisdell JA, and Goldstein JA (1999) Gene structure of CYP2C8 and extrahepatic distribution of the human CYP2Cs. *J Biochem Mol Toxicol* **13**:289–295.

Melet A, Marques-Soares C, Schoch GA, Macherey AC, Jaouen M, Dansette PM, Sari MA, Johnson EF, and Mansuy D (2004) Analysis of human cytochrome P450 2C8 substrate specificity using a substrate pharmacophore and site-directed mutants. *Biochemistry* **43**:15379–15392.

Mück W (1998) Rational assessment of the interaction profile of cerivastatin supports its low propensity for drug interactions. *Drugs* **56 (Suppl 1)**:15–23.

Nadin L and Murray M (1999) Participation of CYP2C8 in retinoic acid 4-hydroxylation in human hepatic microsomes. *Biochem Pharmacol* **58**:1201–1208.

Nakajima M, Fujiki Y, Noda K, Ohtsuka H, Ohkuni H, Kyo S, Inoue M, Kuroiwa Y, and Yokoi T (2003) Genetic polymorphisms of CYP2C8 in Japanese population. *Drug Metab Dispos* **31**:687–690.

Ohyama K, Nakajima M, Nakamura S, Shimada N, Yamazaki H, and Yokoi T (2000) A significant role of human cytochrome P450 2C8 in amiodarone N-deethylation: an approach to predict the contribution with relative activity factor. *Drug Metab Dispos* **28**:1303–1310.

Projean D, Baune B, Farinotti R, Flinois JP, Beaune P, Taburet AM, and Ducharme J (2003) In vitro metabolism of chloroquine: identification of CYP2C8, CYP3A4, and CYP2D6 as the main isoforms catalyzing N-desethylchloroquine formation. *Drug Metab Dispos* **31**:748–754.

Rahman A, Korzekwa KR, Grogan J, Gonzalez FJ, and Harris JW (1994) Selective biotransformation of taxol to 6 alpha-hydroxytaxol by human cytochrome P450 2C8. *Cancer Res* **54**:5543–5546.

Schoch GA, Yano JK, Wester MR, Griffin KJ, Stout CD, and Johnson EF (2004) Structure of human microsomal cytochrome P450 2C8. Evidence for a peripheral fatty acid binding site. *J Biol Chem* **279**:9497–9503.

Schwarz D, Kisselev P, Honeck H, Cascorbi I, Schunck WH, and Roots I (2001) Co-expression of human cytochrome P4501A1 (CYP1A1) variants and human NADPH-cytochrome P450 reductase in the baculovirus/insect cell system. *Xenobiotica* **31**:345–356.

Soyama A, Saito Y, Hanioka N, Murayama N, Nakajima O, Katori N, Ishida S, Sai K, Ozawa S, and Sawada J (2001) Non-synonymous single nucleotide alterations found in the CYP2C8 gene result in reduced in vitro paclitaxel metabolism. *Biol Pharm Bull* **24**:1427–1430.

Soyama A, Saito Y, Komamura K, Ueno K, Kamakura S, Ozawa S, and Sawada J (2002) Five novel single nucleotide polymorphisms in the CYP2C8 gene, one of which induces a frameshift. *Drug Metab Pharamacokinet* **17**:373–377.

Taniguchi R, Kumai T, Matsumoto N, Watanabe M, Kamio K, Suzuki S, and Kobayashi S (2005) Utilization of human liver microsomes to explain individual differences in paclitaxel metabolism by CYP2C8 and CYP3A4. *J Pharmacol Sci* **97**:83–90.

Zeldin DC, Moomaw CR, Jesse N, Tomer KB, Beetham J, Hammock BD, and Wu S (1996) Biochemical characterization of the human liver cytochrome P450 arachidonic acid epoxygenase pathway. *Arch Biochem Biophys* **330**:87–96.

Address correspondence to: Hideto Jinno, Division of Environmental Chemistry, National Institute of Health Sciences, 1-18-1 Kamiyoga, Setagaya-ku, Tokyo 158-8501, Japan. E-mail: jinno@nihs.go.jp

VOLUME 23 · NUMBER 6 · FEBRUARY 20 2005

JOURNAL OF CLINICAL ONCOLOGY

ORIGINAL REPORT

Randomized Pharmacokinetic and Pharmacodynamic Study of Docetaxel: Dosing Based on Body-Surface Area Compared With Individualized Dosing Based on Cytochrome P450 Activity Estimated Using a Urinary Metabolite of Exogenous Cortisol

Noboru Yamamoto, Tomohide Tamura, Haruyasu Murakami, Tatsu Shimoyama, Hiroshi Nokihara, Yutaka Ueda, Ikuo Sekine, Hideo Kunitoh, Yuichiro Ohe, Tetsuro Kodama, Mikiko Shimizu, Kazuto Nishio, Naoki Ishizuka, and Nagahiro Saijo

From the Division of Internal Medicine, National Cancer Center Hospital; Pharmacology Division and Cancer Information and Epidemiology Division, National Cancer Center Research Institute, Tokyo, Japan.

Submitted November 7, 2003; accepted August 19, 2004.

Supported in part by a Grant-in-Aid for Cancer Research (9-25) from the Ministry of Health, Labor, and Welfare, Tokyo, Japan.

Presented in part at the 38th Annual Meeting of the American Society of Clinical Oncology, May 18-21, 2002, Orlando, FL.

Authors' disclosures of potential conflicts of interest are found at the end of this article.

Address reprint requests to Tomohide Tamura, MD, Division of Internal Medicine, National Cancer Center Hospital, 5-1-1, Tsukiji, Chuo-ku, Tokyo, 104-0045, Japan; e-mail: ttamura@ncc.go.jp.

0732-183X/05/2306-1061/$20.00

DOI: 10.1200/JCO.2005.11.036

ABSTRACT

Purpose

Docetaxel is metabolized by cytochrome P450 (CYP3A4) enzyme, and the area under the concentration-time curve (AUC) is correlated with neutropenia. We developed a novel method for estimating the interpatient variability of CYP3A4 activity by the urinary metabolite of exogenous cortisol (6-beta-hydroxycortisol [6-β-OHF]). This study was designed to assess whether the application of our method to individualized dosing could decrease pharmacokinetic (PK) and pharmacodynamic (PD) variability compared with body-surface area (BSA) –based dosing.

Patients and Methods

Fifty-nine patients with advanced non–small-cell lung cancer were randomly assigned to either the BSA-based arm or individualized arm. In the BSA-based arm, 60 mg/m^2 of docetaxel was administered. In the individualized arm, individualized doses of docetaxel were calculated from the estimated clearance (estimated clearance = 31.177 + [7.655 × 10^{-4} × total 6-β-OHF] − [4.02 × alpha-1 acid glycoprotein] − [0.172 × AST] − [0.125 × age]) and the target AUC of 2.66 mg/L · h.

Results

In the individualized arm, individualized doses of docetaxel ranged from 37.4 to 76.4 mg/m^2 (mean, 58.1 mg/m^2). The mean AUC and standard deviation (SD) were 2.71 (range, 2.02 to 3.40 mg/L · h) and 0.40 mg/L · h in the BSA-based arm, and 2.64 (range, 2.15 to 3.07 mg/L · h) and 0.22 mg/L · h in the individualized arm, respectively. The SD of the AUC was significantly smaller in the individualized arm than in the BSA-based arm ($P < .01$). The percentage decrease in absolute neutrophil count (ANC) averaged 87.1% (range, 59.0 to 97.7%; SD, 8.7) in the BSA-based arm, and 87.4% (range, 78.0 to 97.2%; SD, 6.1) in the individualized arm, suggesting that the interpatient variability in percent decrease in ANC was slightly smaller in the individualized arm.

Conclusion

The individualized dosing method based on the total amount of urinary 6-β-OHF after cortisol administration can decrease PK variability of docetaxel.

J Clin Oncol 23:1061-1069. © 2005 by American Society of Clinical Oncology

INTRODUCTION

Many cytotoxic drugs have narrow therapeutic windows despite having a large interpatient pharmacokinetic (PK) variability. The doses of these cytotoxic drugs are usually calculated on the basis of body-surface area (BSA). Although several physiologic functions are proportional to BSA, systemic exposure to a drug is only partially related to

this parameter.[1-3] Consequently, a large interpatient PK variability is seen when doses are based on BSA. This large interpatient PK variability can result in undertreatment with inappropriate therapeutic effects in some patients, or in overtreatment with unacceptable severe toxicities in others. Understanding interpatient PK variability is important for optimizing anticancer treatments. Factors that affect PK variability include drug absorption, metabolism, and excretion. Among these factors, drug metabolism is regarded as a major factor causing PK variability. Unfortunately, however, no simple and practical method for estimating the interpatient variability of drug metabolism is available. If drug metabolism in each patient could be predicted, individualized dosing could be performed to optimize drug exposure while minimizing unacceptable toxicity.

Docetaxel is a cytotoxic agent that promotes microtubule assembly and inhibits depolymerization to free tubulin, resulting in the blockage of the M phase of the cell cycle.[4] Docetaxel has shown promising activity against several malignancies, including non–small-cell lung cancer, and is metabolized by hepatic CYP3A4 enzyme.[5-15]

Human CYP3A4 is a major cytochrome P450 enzyme that is present abundantly in human liver microsomes and is involved in the metabolism of a large number of drugs, including anticancer drugs.[16-18] This enzyme exhibits a remarkable interpatient variation in activity as high as 20-fold, which accounts for the large interpatient differences in the disposition of drugs that are metabolized by this enzyme.[19-22] Several noninvasive in vivo probes for estimating the interpatient variability of CYP3A4 activity have been reported and include the erythromycin breath test, the urinary dapsone recovery test, measurement of midazolam clearance (CL), and measurement of the ratio of endogenous urinary 6-beta-hydroxycortisol (6-β-OHF) to free-cortisol (FC).[23-27] The erythromycin breath test and the measurement of midazolam CL are the best validated, and both have been shown to predict docetaxel CL in patients.[28,29] However, neither probe has been used in a prospective study to validate the correlations observed, or to test their utility in guiding individualized dosing.

We developed a novel method for estimating the interpatient variability of CYP3A4 activity by urinary metabolite of exogenous cortisol. The total amount of 24-hour urinary 6-β-OHF after cortisol administration (total 6-β-OHF) is significantly correlated with docetaxel CL, which is metabolized by the CYP3A4 enzyme. We also illustrate the possibility that individualized dosing to optimize drug exposure and decrease interpatient PK variability could be performed using this method.[30]

We conducted a prospective, randomized PK and pharmacodynamic (PD) study of docetaxel comparing BSA-based dosing and individualized dosing based on the interpatient variability of CYP3A4 activity, as estimated by a urinary metabolite of exogenous cortisol. The objective of this study was to assess whether the application of our method to individualized dosing could decrease PK and PD variability of docetaxel compared with BSA-based dosing.

PATIENTS AND METHODS

Patient Selection

Patients with histologically or cytologically documented advanced or metastatic non–small-cell lung cancer were eligible for this study. Other eligibility criteria included the following: age $\geq$ 20 years; Eastern Cooperative Oncology Group performance status of 0, 1, or 2; 4 weeks of rest since any previous anticancer therapy; and adequate bone marrow (absolute neutrophil count [ANC] $\geq$ 2,000/μL and platelet count $\geq$ 100,000/μL), renal (serum creatinine level $\leq$ 1.5 mg/dL), and hepatic (serum total bilirubin level $\leq$ 1.5 mg/dL, AST level $\leq$ 150 U/L, and ALT level $\leq$ 150 U/L) function. Written informed consent was obtained from all patients before enrollment onto the study.

The exclusion criteria included the following: pregnancy or lactation; concomitant radiotherapy for primary or metastatic sites; concomitant chemotherapy with any other anticancer agents; treatment with steroids or any other drugs known to induce or inhibit CYP3A4 enzyme[17]; serious pre-existing medical conditions, such as uncontrolled infections, severe heart disease, diabetes, or pleural or pericardial effusions requiring drainage; and a known history of hypersensitivity to polysorbate 80. This study was approved by the institutional review board of the National Cancer Center.

Pretreatment and Follow-Up Evaluation

On enrollment onto the study, a history and physical examination were performed, and a complete differential blood cell count (including WBC count, ANC, hemoglobin, and platelets), and a clinical chemistry analysis (including serum total protein, albumin [ALB], bilirubin, creatinine, AST, ALT, gamma-glutamyltransferase, alkaline phosphatase [ALP], and alpha-1 acid glycoprotein [AAG]) were performed. Blood cell counts and a chemistry analysis except for AAG were performed at least twice a week throughout the study. Tumor measurements were performed every two cycles, and antitumor response was assessed by WHO standard response criteria. Toxicity was evaluated according to the National Cancer Institute Common Toxicity Criteria (version 2.0).

Study Design

This study was designed to assess whether the application of our method to individualized dosing could decrease PK and PD variability compared with BSA-based dosing. The primary end point was PK variability and the secondary end point was PD variability (ie, toxicity). In our previous study involving 29 patients who received 60 mg/m^2 of docetaxel, the area under the concentration-time curve (AUC) was calculated to be 2.66 $\pm$ 0.91 (mean $\pm$ standard deviation [SD]) mg/L $\cdot$ h.[30] We assumed that the variability of AUC, represented by the SD, could be reduced by 50% in the individualized arm compared with that in the BSA-based arm, and that AUC would be normally distributed. The required sample size was 25 patients per arm to detect this difference with a two-sided F test at α = .05 and a power of 0.914.

Patients were randomly assigned to either the BSA-based arm or individualized arm (Fig 1). In the BSA-based arm, each patient received a dose of 60 mg/m^2 of docetaxel. In the individualized arm, individualized doses of docetaxel were calculated from the estimated docetaxel CL after cortisol administration and the target AUC (described in the Docetaxel Administration section).

Cortisol Administration and Urine Collection

In the individualized arm, 300 mg of hydrocortisone (Banyu Pharmaceuticals Co, Tokyo, Japan) was diluted in 100 mL of 0.9%

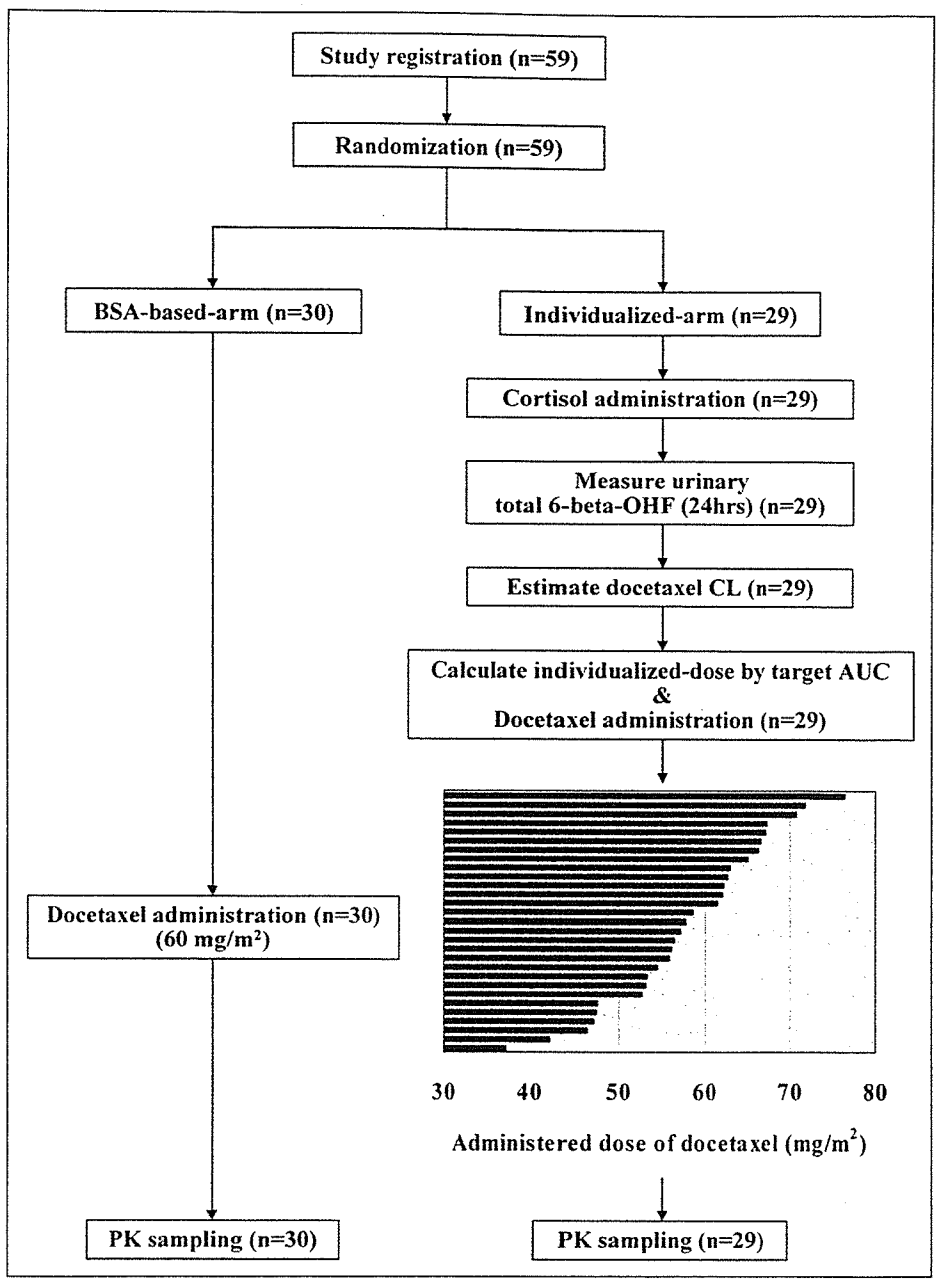

Fig 1. Study flow diagram and administered dose of docetaxel. PK, pharmacokinetic; AUC, area under the concentration-time curve; CL, clearance; 6-β-OHF, 6-beta-hydroxycortisol.

saline and administered intravenously for 30 minutes at 9 AM on day 1 in all patients to estimate the interpatient variability of CYP3A4 activity. After cortisol administration, the urine was collected for 24 hours. The total volume of the 24-hour collection was recorded, and a 5-mL aliquot was analyzed immediately.

Docetaxel Administration

Docetaxel (Taxotere; Aventis Pharm Ltd, Tokyo, Japan) was obtained commercially as a concentrated sterile solution containing 80 mg of the drug in 2 mL of polysorbate 80. In the BSA-based arm, a dose of 60 mg/m^2 of docetaxel was diluted in 250 mL of 5% glucose or 0.9% saline and administered by 1-hour intravenous infusion at 9 AM to all patients.

In the individualized arm, individualized dose of docetaxel was calculated from the estimated CL and the target AUC of 2.66 mg/L · h using the following equations:

$$\text{Estimated CL (L/h/m}^2) = 31.177 + (7.655 \times 10^{-4} \times \text{total-6-}\beta\text{-OHF [}\mu\text{g/d]}) - (4.02 \times \text{AAG [g/L]}) - (0.172 \times \text{AST [U/L]}) - (0.125 \times \text{age [years]})^{30}$$

$$\text{Individualized dose of docetaxel (mg/m}^2) = \text{estimated docetaxel CL (L/h/m}^2) \times \text{target AUC (2.66 mg/L} \cdot \text{h)}$$

At least 2 days after cortisol administration, individualized doses of docetaxel were diluted in 250 mL of 5% glucose or 0.9% saline and administered by 1-hour intravenous infusion at 9 AM to each patient. The doses of docetaxel in subsequent cycles of treatment were unchanged, and no prophylactic premedication to protect against docetaxel-related hypersensitivity reactions was administered in either of the treatment arms.

PK Study

Blood samples for PK studies were obtained from all of the patients during the initial treatment cycle. An indwelling cannula was inserted in the arm opposite that used for the drug infusion, and blood samples were collected into heparinized tubes. Blood samples were collected before the infusion; 30 minutes after the start of the infusion; at the end of the infusion; and 15, 30, and 60 minutes and 3, 5, 9, and 24 hours after the end of the infusion. All blood samples were centrifuged immediately at 4,000 rpm for 10 minutes, after which the plasma was removed and the samples were placed in polypropylene tubes, labeled, and stored at −20°C or colder until analysis.

PK parameters were estimated by the nonlinear least squares regression analysis method (WinNonlin, Version 1.5; Bellkey Science Inc, Chiba, Japan) with a weighting factor of 1 per year.[2] Individual plasma concentration-time data were fitted to two- and three-compartment PK models using a zero-order infusion input and first-order elimination. The model was chosen on the basis of Akaike's information criteria.[31] The peak plasma concentration (C_{max}) was generated directly from the experimental data. AUC was extrapolated to infinity and determined based on the best-fitted curve; this measurement was then used to calculate the absolute CL (L/h), defined as the ratio of the delivered dosage (in milligrams) and AUC.

To assess PD effect of docetaxel, the percentage decrease in ANC was calculated according to the following formula: % decrease in ANC = (pretreatment ANC − nadir ANC)/(pretreatment ANC) × 100.

Measurements

The concentration of urinary 6-β-OHF was measured by reversed phase high-performance liquid chromatography with UV absorbance detection according to previously published methods.[30,32,33]

Docetaxel concentrations in plasma were also measured by solid-phase extraction and reversed phase high-performance liquid chromatography with UV detection according to the previously published method.[30,34] The detection limit corresponded to a concentration of 10 ng/mL.

Statistical Analysis

Fisher's exact test or χ^2 test was used to compare categoric data, and Student's t test was used for continuous variables. The strength of the relationship between the estimated docetaxel CL and the observed docetaxel CL was assessed by least squares linear regression analysis. The interpatient variability of AUC for each arm was evaluated by determining the SD and was compared by F test. Biases, or the mean AUC value in each arm minus the target AUC (2.66 mg/L · h), were also compared between the arms by Student's t test.

A two-sided P value of ≤ .05 or less was considered to indicate statistical significance. All statistical analyses were performed using SAS software version 8.02 (SAS Institute, Cary, NC).

RESULTS

Patient Characteristics

Between October 1999 and May 2001, 59 patients were enrolled onto the study and randomly assigned to either the BSA-based arm (n = 30) or the individualized arm (n = 29). All 59 patients were assessable for PK and PD analyses. The pretreatment characteristics of the 59 patients are listed in Table 1. The baseline characteristics were well balanced between the arms except for three laboratory parameters: ALB, AAG, and ALP. These three parameters were not included in the eligibility criteria. The majority of patients (95%) had a performance status of 0 or 1. Twenty (67%) and 16 (55%) patients had been treated with platinum-based chemotherapy in the BSA-based arm and individualized arm, respectively. Only two patients in the individualized arm had liver metastasis, and most of the patients had good hepatic functions.

Individualized Dosing of Docetaxel

In the individualized arm, the total amount of 24-hour urinary 6-β-OHF after cortisol administration (total 6-β-OHF) was 9,179.6 ± 3,057.7 μg/d (mean ± SD), which was similar to the result of our previous study.[30] The estimated docetaxel CL was 21.9 ± 3.5 L/h/m^2 (mean ± SD), and individualized dose of docetaxel ranged from 37.4 to 76.4 mg/m^2 (mean, 58.1 mg/m^2; Fig 1).

PK

Docetaxel PK data were obtained from all 59 patients during the first cycle of therapy, and PK parameters are listed in Table 2. Drug levels declined rapidly after infusion and could be determined to a maximum of 25 hours. The concentration of docetaxel in plasma was fitted to a biexponential equation, which was consistent with previous reports.[30,35-38] The mean alpha and beta half-lives were 9.2 minutes and 5.0 hours in the BSA-based arm and 9.2 minutes and 7.4 hours in the individualized arm, respectively.

In the BSA-based arm, docetaxel CL was 22.6 ± 3.4 L/h/m^2 (mean ± SD), and AUC averaged 2.71 mg/L · h (range, 2.02 to 3.40 mg/L · h). In the individualized arm, docetaxel CL was 22.1 ± 3.4 L/h/m^2, and AUC averaged 2.64 mg/L · h (range, 2.15 to 3.07 mg/L · h). The least squares linear regression analysis showed that the observed docetaxel CL was well estimated in the individualized arm (r^2 = 0.821; Fig 2).

The SDs of AUC in the BSA-based arm and in the individualized arm were 0.40 and 0.22, respectively, and the ratio of SD in the individualized arm to that in the BSA-based arm was 0.538 (95% CI, 0.369 to 0.782). The biases from the target AUC in the BSA-based arm and in the individualized arm were 0.047 (95% CI, −0.104 to 0.198) and −0.019 (95% CI, −0.102 to 0.064), respectively, with no significant difference. The interpatient variability of